Vorträge für Pflanzenzüchtung
Heft 89 2023

20. Kurt von Rümker-Vorträge

Quedlinburg, 04. bis 05. Oktober 2023

Gesellschaft für Pflanzenzüchtung e. V.

Erschienen:	Dezember 2023
Erhältlich durch:	GPZ-Geschäftsstelle Erwin-Bauer-Straße 27, 06484 Quedlinburg
ISSN-Nr.:	0723 – 7812
Seiten gesamt:	65

Inhalt

20. Kurt von Rümker-Vorträge 2023

Vorwort

Kurt von Rümker gilt als der Begründer der wissenschaftlichen Pflanzenzüchtung in Deutschland. In Erinnerung an sein Lebenswerk verleiht die Gesellschaft für Pflanzenzüchtung alle zwei Jahre den Kurt-von-Rümker Preis für den besten Vortrag einer Nachwuchswissenschaftlerin oder eines Nachwuchswissenschaftlers auf dem Gebiet der Pflanzenzüchtung. Das vorliegende Heft beinhaltet die im Rahmen der 7. Quedlinburger Pflanzenzüchtungstage gehaltenen Vorträge für den 20. Kurt von Rümker-Preis.

Der dreiköpfigen Jury, bestehend aus Prof. Dr. Klaus Pillen, Dr. Janine König und Michael Koch fiel die schwierige Aufgabe zu, unter den hervorragenden Präsentationen einen Preisträger auszuwählen. Hierfür gebührt ihnen unser herzlicher Dank.

Der Preis, der seit 1985 zur Förderung des wissenschaftlichen Nachwuchses auf dem Gebiet der Pflanzenzüchtung verliehen wird, ist mit 2.500 Euro dotiert. Zusätzlich erhält der Gewinner eine einjährige Mitgliedschaft in der EUCARPIA, der Europäischen Fachgesellschaft für Pflanzenzüchtung. Der Preis ging dieses Jahr an Dr. Thomas Bergemann von NPZ, Holtsee. Herr Bergmann setzte sich mit seinem Vortrag über die Identifikation neuer Resistenzgene gegen die Wurzelhals- und Stängelfäule in Winterraps gegen seine acht Mitbewerberinnen und Mitbewerber durch.

Den Rahmen für die Kurt von Rümker-Vorträge bildete in diesem Jahr eine Fachtagung zum Thema „*Digital Plant Breeding*“. Über 40 Wissenschaftlerinnen und Wissenschaftler sowie Züchterinnen und Züchter trafen sich in Quedlinburg auf Einladung des Julius Kühn-Instituts (JKI) und der Gesellschaft für Pflanzenzüchtung (GPZ), um sich u.a. über die Nutzung von Digitalisierung und Künstlicher Intelligenz in der Phänotypisierung, Modellierungen und Genomanalyse auszutauschen.

Die Veranstaltung wurde gemeinsam von der GPZ und dem JKI organisiert. An dieser Stelle sei nochmals allen Kurt von Rümker-Vortragenden für ihre Beiträge gedankt, die sie im Folgenden wiederfinden.

GPZ-Präsidentin
Prof. Dr. Maria von Korff Schmising

Gesellschaft für Pflanzenzüchtung e.V.

Zur Erinnerung an die erste akademische Vorlesung über Pflanzenzüchtung 1889 in Göttingen durch den damals 30-jährigen Privatdozenten Dr. Kurt von Rümker verleiht die Gesellschaft für Pflanzenzüchtung e.V. anlässlich ihrer

Vortragstagung vom 4. bis 5. Oktober 2023 in Quedlinburg den

Kurt von Rümker-Preis

für den besten Vortrag eines Nachwuchswissenschaftlers
auf dem Gebiet der Pflanzenzüchtung an

Dr. Thomas Bergmann

von der NPZ Innovation GmbH

Das Thema des Vortrages lautete:

„Identification of a novel allele (Rlm7-3) of the race-specific resistance gene Rlm7 in winter oilseed rape (B. napus) against blackleg (L. maculans) by genetic mapping and functional genomics "

Der Vortrag wird in der Reihe „Vorträge für Pflanzenzüchtung" online veröffentlicht.

Die mit dem Preis verbundene Anerkennung in Höhe von 2.500,00 Euro stiftete die Gesellschaft für Pflanzenzüchtung e.V. (GPZ).

Der Vorstand wünscht dem Preisträger auch in Zukunft beruflich besten Erfolg.

Quedlinburg, den 5. Oktober 2023

Geschäftsführender Vizepräsident

Gesellschaft für Pflanzenzüchtung e. V.
Telefon: 03946/ 47-899
Telefax: 03946/ 47-1002
E-Mail: geschaeftsstelle@gpz-online.de
Homepage: http://www.gpz-online.de
Erwin-Baur-Straße 27
06484 Quedlinburg
Harzsparkasse • BLZ: 810 520 00 • Kontonummer: 331 009 200
IBAN: DE91 8105 2000 0331 0092 00 • BIC: NOLADE21HRZ

Vorträge für Pflanzenzüchtung 89, 1-9, 2023

Identification of a novel allele (Rlm7-3) of the race-specific resistance gene Rlm7 in winter oilseed rape (B. napus) against blackleg (L. maculans) by genetic mapping and functional genomics

Thomas Bergmann

Department of Molecular Phytopathology and Biotechnology, Institute of Phytopathology, Christian-Albrechts-University of Kiel, 24118 Kiel, Germany

Present address: NPZ Innovation GmbH, Hohenlieth-Hof, 24363 Holtsee

Introduction

Brassica napus (oilseed rape) belongs to the most important oilseed crops worldwide. *Leptosphaeria maculans*, causal agent of the blackleg disease (syn. Phoma stem canker), causes severe yield losses in many oilseed rape areas with special concern in Europe, Canada, and Australia. Two types of resistance against *L. maculans* are effective in oilseed rape: qualitative and quantitative resistance (Delourme et al. 2006). Qualitative resistance is controlled by single resistance (R) genes that are effective against certain races of *L. maculans*. In contrast to qualitative resistance, quantitative resistance is controlled by several genes and effective against a broad spectrum of races. Qualitative resistance provides complete protection against seedling infection, the main cause for severe yield losses in oilseed rape due to blackleg. Quantitative resistance, on the other hand, provides partial protection of the host throughout its complete life cycle and especially in its adult phase. Since heavy yield losses are prevented by qualitative resistance, breeding resistant varieties against *L. maculan*s remains a key strategy to counteract blackleg epidemics (Fitt et al. 2006). More than 15 R genes have been described in Brassica germplasm against blackleg of which the *Rlm7* locus represents one of the most important *B. napus* race-specific resistance genes against the disease in Europe (Alnajar et al. 2022, Mitrousia et al., 2018, van de Wouw et al. 2020). *Rlm7* confers seedling resistance against races of *L. maculans* with the avirulence (Avr) gene *AvrLm7*. The *Rlm7* locus was originally mapped to a cluster with *Rlm3*/*4*/*9* on chromosome A07 and it was hypothesized that these R genes are allelic variants of the same locus (Delourme et al. 2004, Larkan et al. 2016). Recently, it was proven that *Rlm7* is an allelic variant of *Rlm9* encoding for a wall-associated kinase-like (WAKL) protein (Haddadi et al. 2022, Larkan et al. 2020). Here, we report the genome-based identification and molecular characterization of a novel allele of *Rlm7*, referred to as *Rlm7-3*, in winter oilseed rape (*B. napus*) against blackleg (*L. maculans*).

For this, the *Rlm7-AvrLm7* pathosystem was established for identifying suitable genotypes for genetic mapping and for studying the *B. napus – L. maculans* interaction in more detail. The genetic analysis was complemented by transcriptomics and functional genomics for candidate gene identification. The successful identification of *Rlm7-3* provides new insights into the *Rlm7-AvrLm7* interaction and a working model for the resistance gene identification in polyploid crops.

Characterization of the *Rlm7-AvrLm7* pathosystem in *B. napus*

A set of defined *B. napus* genotypes and isolates of *L. maculans* was used for establishment of the *Rlm7-AvrLm7* pathosystem. The material was provided by the NPZ Innovation GmbH (NPZi; Holtsee, Germany) of which three genotypes and two isolates were in the focus of this study. One genotype, denoted as Bn1, carries the *Rlm7* locus while the other two genotypes (Bn4, Bn5) carry no R genes relevant for this study and were used as susceptible controls. The Lm17 isolate carries the corresponding Avr gene *AvrLm7* and the Lm106 isolate carries the *AvrLm3* gene. The varieties Columbus (*Rlm1*, *Rlm3*), Bristol (*Rlm2*, *Rlm9*), and Darmor (*Rlm9*) were included as reference genotypes. Phenotypes were assessed by infection of 7-day old seedlings by point-inoculation of cotyledons according to Zhang et al. (2016). The cotyledon inoculation of the *B. napus* set demonstrated a race-specific interaction between Bn1 (*Rlm7*) and Lm17 (*AvrLm7*). As shown in Figure 1, pronounced disease symptoms emerged in the susceptible lines Bn4 and Bn5 as well as in Columbus (*Rlm1, Rlm3*), Bristol (*Rlm2*, *Rlm9*), and Darmor (*Rlm9*) when infected with the isolate Lm17 (*AvrLm7*) but not in the resistant Bn1 (*Rlm7*) plant at all. Correspondingly, Bn1 was susceptible to the isolate Lm106 (*AvrLm3*) whereas Columbus showed resistance against this isolate. The point-inoculation system of the cotyledons showed a clear separation of resistant and susceptible phenotypes as expected by their genotypes. In contrast to other bioassays, the cotyledon inoculation system is a very robust and reliable method to study the *B. napus – L. maculans* pathosystem.

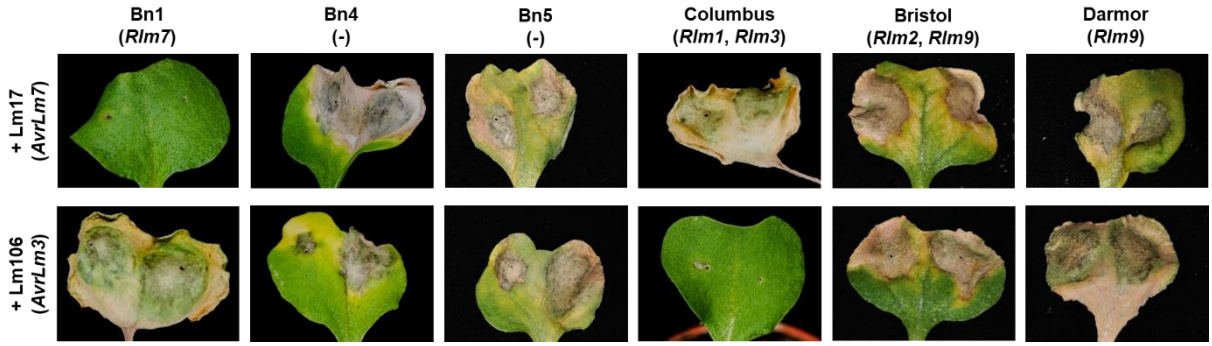

Figure 1 Phenotypical characterization of *B. napus* genotypes in response to two *L. maculans* isolates (Lm17, Lm106). Seven-day old cotyledons were point-inoculated based on Zhang et al. (2016). Pictures were taken 19 days post inoculation (dpi).

Genetic mapping of the *Rlm7* locus and candidate gene identification

Two double haploid (DH) populations (110 individuals each population) were generated from crosses of Bn1 (*Rlm7*) with Bn4 and Bn5, referred to as Population A and B. The populations were screened for their phenotypes by point-inoculation of cotyledons with *L. maculans* isolate Lm17 (*AvrLm7*). Genotyping was conducted with the 15k Brassica SNP-chip assay carried out by SGS TraitGenetics (Gatersleben, Germany). Genetic map construction and QTL analysis was carried out with R/qtl (Broman et al. 2003). Marker sequences were assigned physical genome positions via a BLAST search against the Darmor-bzh reference genome (Rousseau-Gueutin et al. 2020) and against long read sequencing data of Bn1 provided by the NPZi. The single-QTL scan identified one major QTL in each population explaining 52 % and 68 % of phenotypical variance, respectively. Based on the Darmor-bzh reference genome, which carries the *Rlm9* locus, the QTL is located on chromosome A07 between 19.5 mbp and 20.6 mbp (Table 1). This region is overlapping with the *Rlm3*/*4*/*7*/*9* cluster and the QTL peak (LOD = 26.9) was pointing to the location of the *Rlm9* locus that was cloned in Darmor-bzh by Larkan et al. (2020).

Table 1 Identified QTL for *Rlm7* and its genomic position in Darmor-bzh and Bn1 (contig_9)

Population	Marker/Pseudomarker	Linkage group	cM	LOD	Position [bp]	
					Darmor-bzh [v. 10]	contig_9
Population A (Bn1 x Bn4)	**Bn-A07-p13323913**	A07	45.59	9.1	19,563,046	1,569,984
	cA07.loc46	A07	46.00	9.6	-	-
	…	…	…	…	…	…
	cA07.loc51	A07	51.00	15.7	-	-
	Bn-A07-p13787534	A07	51.72	16.2	20,021,188	2,123,566
	Bn-A07-p13844810	A07	51.72	16.2	20,079,904	2,052,249
	cA07.loc52	A07	52.00	16.1	-	-
	Bn-scaff_15818_1-p2331085	A07	52.69	15.1	20,150,162	2,174,961
	cA07.loc53	A07	53.00	15.3	-	-
	Bn-A07-p14002586	A07	53.66	15.1	20,215,550	2,253,382
	Bn-A07-p14129550	A07	53.66	15.1	20,345,927	2,379,176
	cA07.loc54	A07	54.00	14.9	-	-
	Bn-A07-p14382008	A07	54.64	14.1	20,594,536	2,627,483
Population B (Bn1 x Bn5)	**Bn-A07-p13936486**	A07	47.45	26.1	20,155,129	2,176,943
	cA07.loc48	**A07**	**48.00**	**26.9**	**-**	**-**
	cA07.loc49	A07	49.00	26.5	-	-
	Bn-A07-p14026612	A07	49.33	25.9	20,236,964	2,274,803
	Bn-A07-p14103536	A07	49.33	25.9	20,313,843	2,350,139

An *in-silico* screen of the physical region of Darmor-bzh corresponding to the QTL peak proved that *Rlm9* is the only defense-related gene in this region as shown before by Larkan et al. (2020) suggesting that the *Rlm9* locus may be different in a *Rlm7* genotype. To validate this, we used long read sequencing data of the *Rlm7* donor Bn1 for a comparative genome analysis. The QTL was identified on a 4 mbp-long scaffold (contig_9) in the Bn1 genome corresponding to a physical interval of 1.05 mbp. The QTL peak was identified within a 97 kbp interval on contig_9 (Table 1).

Comparative genome analysis revealed a high sequence similarity between the two genomes in this region with most dissimilarities being due to small gaps of less than 100 bp. According to an *in-silico* gene prediction, 21 gene models are located within the QTL peak in the Bn1 genome. All predicted gene models in Bn1 are present in the Darmor-bzh reference genome as well. Strikingly, one gene model in Bn1, encoding for a WAKL, shows high sequence homology to the *Rlm9* locus in the Darmor-bzh genome but with a 6 kbp-long intron and mismatches in the 5' region of the gene. The *in-silico* predicted gene models were confirmed by transcriptome analysis through comparative RNAseq with Lm17-inoculated cotyledons of Bn1 and Bn4 (Figure 2A). The transcriptome data validated the predicted gene structure of the WAKL that was identified in Bn1 and the locus was first named as *Bna.WAKL10.A07a* due to its homology to the *WAKL10* in *A. thaliana*. According to the RNAseq, the WAKL was specifically expressed in Bn1 but not in the susceptible Bn4 genotype (Figure 2B).

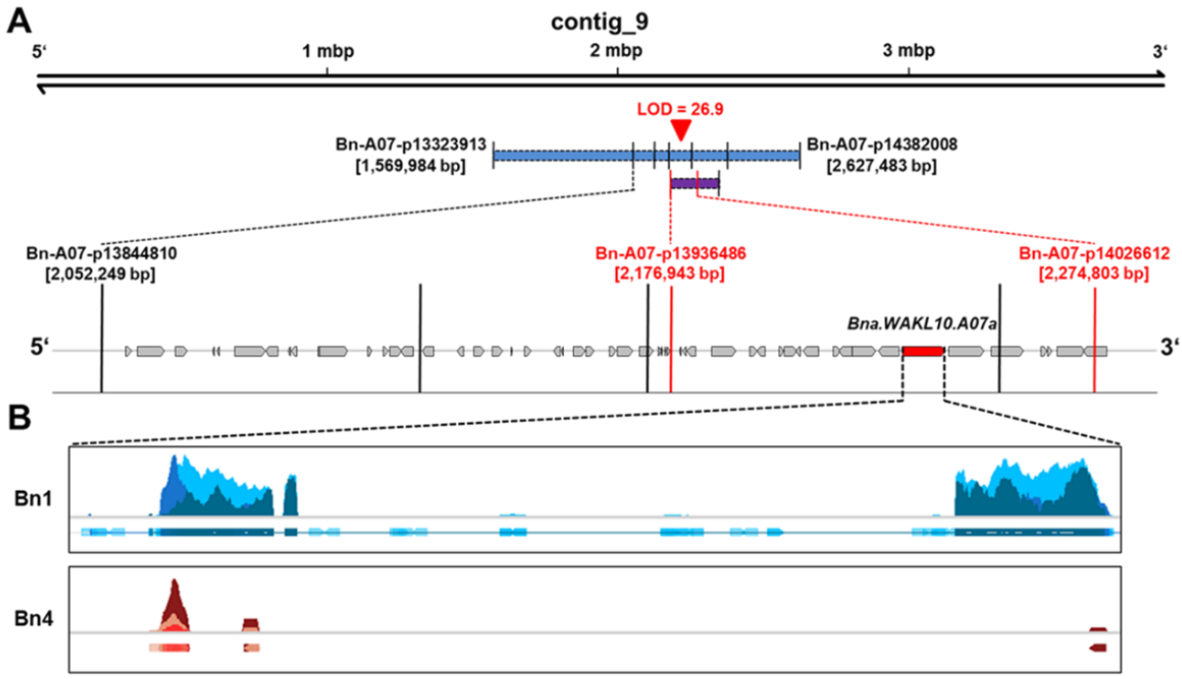

Figure 2: Identification of *Bna.WAKL10A07.a* as candidate for *Rlm7* in German winter oilseed rape. **A** Physical position and gene annotation of the QTL in the genome of Bn1 (*Rlm7*). QTL intervals from Population A and B are highlighted by blue and purple rectangles, respectively. The QTL peak is marked by a red triangle. SNP markers are highlighted by vertical lines and red markers indicate the QTL peak interval. **B** Read coverage of RNAseq from Bn1 (upper track) and Bn4 (lower track) show the gene structure of *Bna.WAKL10A07.a* and its specific expression in Bn1.

The WAKL consists of four exons and has a total transcript length of 3.2 kbp (Figure 3). The open reading frame (ORF) is predicted to feature an extracellular WAK_GUB domain, a WAK domain, an EGF-like calcium domain, a predicted transmembrane domain, and a serine/threonine protein kinase domain. Except for one missing signal

peptide at the N-terminus of the peptide, the WAKL shares the same protein domain structure with the Rlm9 and Rlm7 proteins. The amino acid sequence homology to the Rlm7 protein is 98.7 % and 82.7 % to the Rlm9 protein. The missing signal peptide at the N-terminus of the peptide suggests that the WAKL may be a novel variant of the *Rlm7* locus and named as *Rlm7-3* due to its high sequence homology to the recently cloned alleles (*Rlm7-1*, *Rlm7-2*) of the *Rlm7* locus (Haddadi et al. 2022).

The *Rlm7*-specificity of *Rlm7-3* was confirmed in a diverse set of *B. napus* genotypes. First, its specificity was validated in resistant DH plants from the mapping populations (Figure 4A). Next, its absence was validated in *B. napus* genotypes susceptible to the Lm17 isolate, such as Bn4 and Bn5 (Figure 4B). Finally, we confirmed its specificity in independent *Rlm7* lines from the NPZi and its absence in genotypes with different R genes from the *Rlm3*/*4*/*9* cluster (Figure 4C).

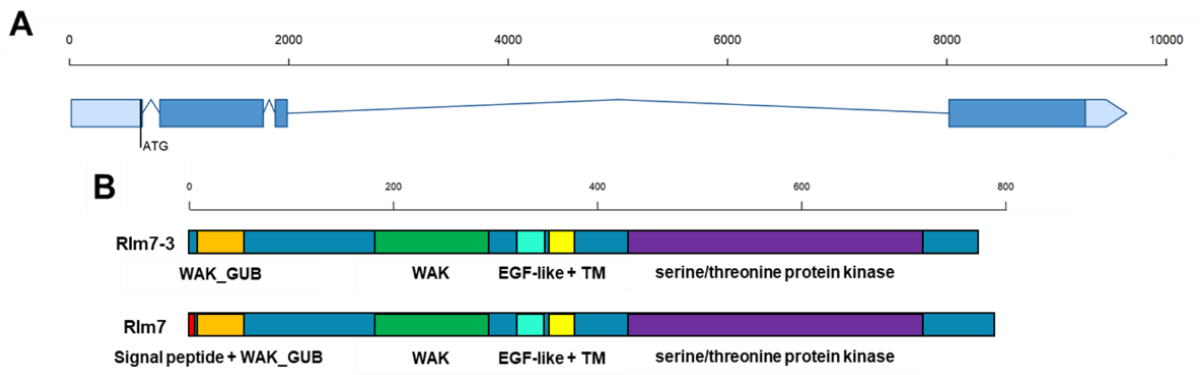

Figure 3 Sequence analysis of *Bna.WAKL10.A07a* (*Rlm7-3*). **A** Schematic transcript structure of *Bna.WAKL10.A07a*. Light blue boxes indicate untranslated regions. Blue boxes indicate translated regions. Introns are indicated by solid lines. **B** Protein structure comparison of Bna.WAKL10.A07a (Rlm7-3) and Rlm7. Top: predicted protein structure of Rlm7-3. Bottom: predicted protein structure of Rlm7 according to Haddadi et al. (2022).

Taken together, we have collected convincing evidence that the identified WAKL is a novel variant of the *Rlm7* locus in winter oilseed rape showing remarkable sequence differences to the published *Rlm7* alleles in summer oilseed rape. This may indicate that the underlying resistance mechanism in winter oilseed rape may differ from the resistance mechanism in summer oilseed rape. The functional validation of *Rlm7-3* by genetic complementation is in progress.

Figure 4 PCR-genotyping of different *B. napus* genotypes for the presence *of Bna.WAKL10.A07a* (*Rlm7-3*). Expected amplicon length is 665 bp. **A** The expected amplicon was produced in Bn1 and in four resistant DH plants from Population A. **B** No specific amplicon was produced in *B. napus* genotypes susceptible to Lm17 (*AvrLm7*). Dar = Darmor (*Rlm9*), Bri = Bristol (*Rlm2*/*9*), Col = Columbus (*Rlm1*/*3*), Exp = Express617 (NA), Wes = Westar (no R genes). **C** Detection of the *Bna.WAKL10.A07a* (*Rlm7-3*) fragment in independent *Rlm7* genotypes. Amplicons were confirmed by sequencing.

Molecular characterization of the *Rlm7*-mediated resistance

Lastly, we focused on the molecular characterization of the *Rlm7*-mediated resistance. For this, we used fluorescence microscopy, real-time quantitative PCR (rt-qPCR), and comparative transcriptomics by RNAseq. The *Rlm7*-mediated resistance by Bn1 was compared with the susceptible interaction between Bn4 and Lm17 throughout different time-points after inoculation. Phenotypical and microscopical analyses indicated a breakpoint in the pathogenesis between 7 to 11 dpi when symptom development emerged in susceptible cotyledons but not in resistant cotyledons.

In this stage, we observed a fast growth and asexual sporulation of the fungus in the susceptible cotyledons that appeared to be completely absent in resistant cotyledons (Figure 5A). The physiological changes of the fungus in susceptible cotyledons coincided with the shift of its biotrophic to its necrotrophic lifestyle during the host-parasite interaction (Haddadi et al. 2016). Gene expression analysis of marker genes for important plant hormones showed that *BnPR1*, marker for salicylic acid (SA), was significantly induced in both interactions but much stronger addressed in the resistant interaction at the early stage (1 dpi to 3 dpi) of the interaction (Figure 5B). Interestingly, the expression of *BnPR1* was significantly higher in the later stage of the interaction from 7 dpi to 11 dpi in susceptible cotyledons compared to resistant cotyledons.

The RNAseq analysis corroborated the strong importance of SA at the early phase of the resistant interaction by showing that SA-associated signaling pathways were highly and stronger upregulated in Bn1 as early as 3 dpi, as well as genes known to be involved in the R gene signaling pathway. On the other hand, expression of *BnETR2*, a marker for ethylene (ET), showed an initial induction of the gene at 1 dpi followed by a continuous increase in expression in both interactions from 3 to 11 dpi. The gene showed no significant differences in expression between both interactions at any time-point (Figure 5B). This aligned well with the pathogen's lifestyle change suggesting that it seems to be contained at the inoculation site in resistant cotyledons throughout the interaction but not suppressed in its physiological change.

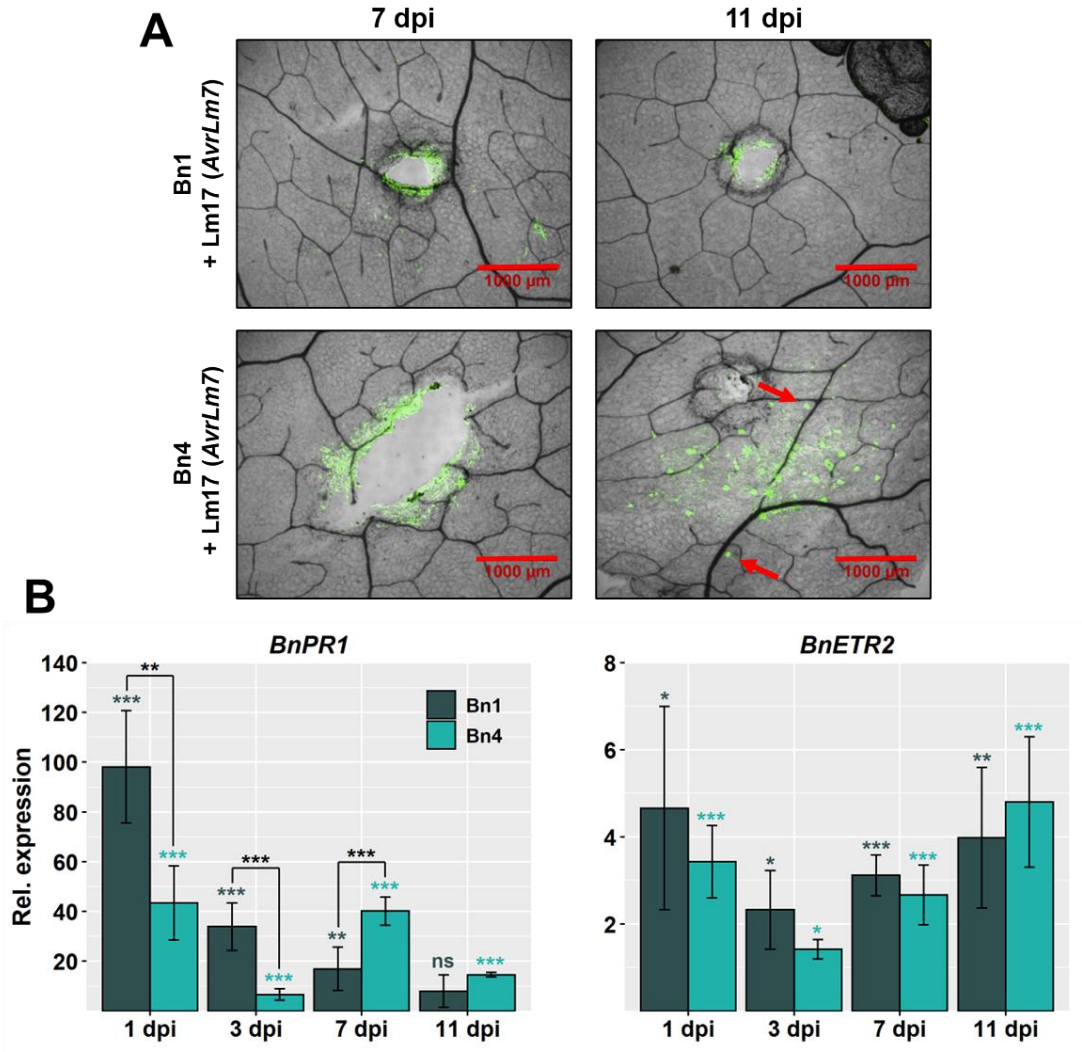

Figure 5 Molecular characterization of the *Rlm7*-mediated resistance. **A** Microscopic analysis of cotyledons of Bn1 and Bn4 inoculated with Lm17 (*AvrLm7*) at 7- and 11-days post inoculation (dpi). Chitin was stained by green fluorescence dye. Red arrows highlight pycnidia formations. **B** Gene expression analysis of the hormone marker genes *BnPR1* (salicylic acid) and *BnETR2* (ethylene) by rt-qPCR at 1, 3, 7, and 11 dpi in cotyledons of Bn1 and Bn4 after inoculation with the Lm17 isolate.

Summary

In this study, we report the identification of a new *Rlm7* allele (*Rlm7-3*) in German winter oilseed rape. *Rlm7-3* shows high homology (98.7 %) to the recently cloned *Rlm7* and misses a signal peptide at the N-terminus of the peptide. This structural difference indicates that the resistance mechanism by *Rlm7-3* may differ from *Rlm7-1* and *Rlm7-2* by Haddadi et al. (2022). The functional validation of *Rlm7-3* by genetic complementation in winter oilseed rape is in progress. Further, our data indicates a breakpoint in the pathogenesis between 7 dpi to 11 dpi, when the pathogen transitions from its biotrophic to its necrotrophic lifestyle. The resistance mechanism of *Rlm7-3* is associated with a significant expression of SA-associated genes at the early phase of the interaction (1 dpi to 3 dpi) and seems to contain the fungus at the inoculation site. The identification of *Rlm7-3* provides novel insights into the *Rlm7-AvrLm7* pathosystem and helps in breeding resistant *B. napus* varieties against *L. maculans*.

Acknowledgments

The authors would like to thank Dr. Falk Hubertus Behrens, Zheng Zhou, Christin Thiele-Belz, Lena Ladewig and Tabea Meyer for their technical assistance. Also, we thank Dr. Steffen Rietz and Dr. Gunhild Leckband from the NPZi for providing us plant and sequencing material. We thank the Stiftung Schlewsig-Holsteinische Landschaft for providing scholarship to Thomas Bergmann (2018/06), and DAAD and BLE for travel grants. This work was financially supported by the BMBF (Grant no. 0315637 B), the BMEL and the FNR (Grant no. 22006516).

Literature

Alnajar D, von Tiedemann A, Koopmann B (2022) Efficacy of blackleg major resistance genes in *B. napus* in Germany. *Pathogens* 11(4):461

Broman KW, Wu H, Sen S, Churchill GA (2003) R/qtl: QTL mapping in experimental crosses. *Bioinformatics* 19(7):889-890

Delourme R, Chevre AM, Brun H, Rouxel T, Balesdent MH, Dias JS, Salisbury P, Renard M, Rimmer SR (2006) Major gene and polygenic resistance to *Leptosphaeria maculans* in oilseed rape (*Brassica napus*). *European Journal of Plant Pathology* 114:41-52

Delourme R, Pilet-Nayel ML, Archipiano M, Horvais R, Tanguy X, Rouxel T, Brun H, Renard M, Balesdent MH (2004) A cluster of major specific resistance genes to *Leptosphaeria maculans* in *Brassica napus*. *Phytopathology* 94:578-583

Fitt BDL, Brun H, Barbetti MJ, Rimmer SR (2006) World-wide importance of Phoma stem canker (*Leptosphaeria maculans* and *L. biglobosa*) on oilseed rape (*Brassica napus*). *European Journal of Plant Pathology* 114:3-15

Haddadi P, Larkan NJ, van de Wouw A, Zhang Y, Neik TX, Beynon E, Bayer P, Edwards D, Batley J, Borhan MH (2022) Brassica napus genes *Rlm4* and *Rlm7*, conferring resistance to *Leptosphaeria maculans*, are alleles of the *Rlm9* wall-associated kinase-like resistance locus. *Plant Biotechnology Journal* 20(7):1229-1231

Haddadi P, Ma L, Wang H, Borhan MH (2016) Genome-wide transcriptomic analyses provide insights into the lifestyle transition and effector repertoire of *Leptosphaeria maculans* during the colonization of *Brassica napus* seedlings. *Molecular Plant Pathology* 17:1196-1210

Larkan NJ, Ma L, Haddadi P, Buchwaldt M, Parkin IAP, Djavaheri M, Borhan MH (2020) The *Brassica napus* wall-associated kinase-like (WAKL) gene *Rlm9* provides race-specific blackleg resistance. *The Plant Journal* 104:892-900

Larkan NJ, Yu F, Lydiate DJ, Rimmer SR, Borhan MH (2016) Singe R gene introgression lines for accurate dissection of the *Brassica – Leptosphaeria* pathosystem. *Frontiers in Plant Science* 7:1771

Mitrousia GK, Huang YJ, Qi A, Sidique SNM, Fitt BDL (2018) Effectiveness of *Rlm7* resistance against *Leptosphaeria maculans* (phoma stem canker) in UK winter oilseed rape cultivars. *Plant Pathol* 67:1339-1353

Rousseau-Gueutin M, Belser C, Da Silva C, Richard G, Istace B, Cruaud C, Falentin C, Boideau F, Bouette J, Delourme R, Deniot G, Engelen S, Ferreira de Carvalho J, Lemainque A, Maillet L, Morice J, Wincker P, Denoeud F, Chevre AM, Aury JM (2020) Long-read assembly of the *Brassica napus* reference genome Darmor-bzh. *GigaScience* 9:1-16

van de Wouw AP, Howlett BJ (2020) Advances in understanding the *Leptosphaeria maculans – Brassica* pathosystem and their impact on disease management. *Canadian Journal of Plant Pathology* 42:149-163

Zhang X, Peng G, Kutcher HR, Balesdent MH, Delourme R, Fernando WGD (2016) Breakdown of *Rlm3* resistance in the *Brassica napus – Leptosphaeria maculans* pathosystem in western Canada. *Eur J Plant Pathol* 145:659-674

Vorträge für Pflanzenzüchtung 89, 11-15, 2023

Genom-Editierung von Branched head in Weizen – Erweiterung der genetischen Diversität mit Potential für Ertragssteigerungen durch veränderte Ährenarchitektur

Christian Hertig
Leibniz-Institut für Pflanzengenetik und Kulturpflanzenforschung (IPK),
Corrensstr. 3, 06466 Seeland OT Gatersleben

Einleitung

Weizen (*Triticum aestivium* L.) stellt eine der wichtigsten Getreidearten dar, nimmt im Vergleich der Kulturpflanzen weltweit die größte Anbaufläche ein und ergibt damit die zweitgrößte Produktionsmenge (FAOSTAT 2019). Ein wichtiges züchterisches Ziel stellt die Steigerung des Ertrages dar, welche eine essentielle Komponente zur Sicherung der Nahrungsversorgung in den nächsten Dekaden ist (Ray et al., 2013). Der Ertrag ist unter anderem abhängig von den Ährenertragskomponenten Kornzahl, Korngröße bzw. -masse sowie von den für die Kornfüllung zur Verfügung stehenden Nährstoffen. Züchterisch erfolgte die Steigerung des Ertrages durch Selektion, Kreuzungen sowie ungerichtet induzierte Mutagenese. In diese Reihe fügt sich die Nutzung Zielsequenz-spezifizierter Endonukleasen ein, wodurch eine gerichtet induzierte Mutagenese zur gezielten Veränderung bestimmter Eigenschaften möglich ist. Die derzeit populärsten molekularen Werkzeuge dafür sind die *guide* (g)RNA-geleiteten Cas9-Endonukleasen, welche in einem durch die gRNA adressierbaren genomischen Zielmotiv einen Doppelstrangbruch der DNA erzeugen, bei dessen zellulärer Reparatur Fehler in Form von Mutationen entstehen können.

Mit Hilfe dieser Technik sollte die Mutagenese des zur APETALA2/ETHYLENE RESPONSE FACTOR (AP2/ERF) Transkriptionsfaktorfamilie gehörenden Gens *Branched head (Bh)* - auch bekannt als *Wheat frizzy panicle (Wfzp)* - induziert werden. Dieser Faktor wurde in den vergangenen zehn Jahren recht gut beschrieben, da er eine Hauptkomponente für die Regulation der Ährenentwicklung ist (Li et al., 2021). Ein Aminosäuretausch im A-Homoeoallel von *Branched head* wurde in verschiedenen Akzessionen des sog. „Wunderweizens“ *T. turgidum convar. compositum* (L.f.) Filat. beschrieben, wodurch es zur Verzweigung der Ähre kommt und deutlich mehr Körner pro Ähre gebildet werden (Poursarebani et al., 2015). In hexaploidem Weizen wurden ebenfalls verschiedene Mutationen in den Homöoallelen der A- und D-Subgenome beschrieben, welche die Bildung überzähliger Ährchen und eine erhöhte Kornzahl verursachen (Dobrovolskaya et al., 2015).

Ziel dieser Studie war die Generierung modifizierter Allele aller drei subgenomischen Kopien von *Branched head* und die Untersuchung der durch einzelne und kombinierte Mutationen resultierenden phänotypischen Veränderungen.

Material und Methoden

Klonierung, Pflanzenmaterial und Transformation

Die zielmotivspezifischen gRNA/*cas9*-Vektoren enthalten Expressionskassetten für jeweils eine gRNA unter Kontrolle des Weizen *U6*-Promotors, für *cas9* unter Kontrolle des Mais *POLYUBIQUITIN 1*-Promotors sowie das für die Pflanzenselektion mit Hygromycin benötigte Resistenzgen *hygromycinphosphotransferase*. Es wurden zwei Zielmotive (ZM 4 und 5), innerhalb bzw. hinter der AP2-Domäne liegend, ausgewählt.

Zur Transformation wurde der Sommerweizen *T. aestivum* Zuchtlinie Bobwhite verwendet. Dessen auf Eis geerntete, unreife Karyopsen wurden mittels Natriumhypochlorit sterilisiert und gewaschen. Die anschließende Transformation erfolgte mittels ballistischem DNA-Transfer in Anlehnung an Ismagul et al. (2014) mit einigen Modifikationen (Hertig 2023). Hierfür wurden beide gRNA/*cas9*-Vektoren gemeinsam an Goldpartikeln präzipitiert und ballistisch in Zellen unreifer Embryonen überführt. Während der anschließenden Kallusbildung und Pflanzenregeneration erfolgte eine Selektion mittels Hygromycin.

Genotypische und phänotypische Analyse der Regenerate und deren Nachkommen

Die in allen drei Homoeoallelen vorhandenen Zielregionen wurden in den regenerierten Pflanzen mittels Subgenom-spezifischer Oligonukleotide amplifiziert und über Sanger-Sequenzierung analysiert. Nachkommen der Primärregenerate wurden durch Selbstbefruchtungen, Kreuzungen und die Herstellung Doppelhaploider (Hertig, 2023) erzeugt und sequenziert. Insgesamt wurden bis zu fünf Generationen untersucht, um homozygot-mutierte Pflanzen zu erhalten.

Zur Ermittlung äußerlicher Veränderungen der mutierten Pflanzen wurden verschiedene Parameter der in Einzeltöpfen wachsenden Pflanzen bestimmt - unter anderem die Zahl der gebildeten Ährchen und der Körner pro Ähre, die Kornbreite und die Tausendkornmasse (TKM). Der Kornertrag pro Ähre und Pflanze wurde wie folgt berechnet: Kornertrag/Ähre = (TKM*Körner/Ähre)/1000; Kornertrag/Pflanze = Kornertrag/Ähre*Ährenzahl

Das Wurzelwachstum wurde über 44 Tage in einem *LemnaTec*-System für mittlere bis große Pflanzen in spezifischen Wurzelphänotypisierungstöpfen beobachtet und dokumentiert. Die Länge und Verzweigung der Wurzeln wurde unter Verwendung der Bildanalysesoftware *saRIA* (Narisetti et al., 2019) ausgewertet.

Ergebnisse

Der ballistische Gentransfer der zwei spezifischen gRNA/*cas9*-Vektoren erfolgte anhand von 1200 Weizenembryonen und erbrachte sieben mutierte Pflanzen. In vier dieser mutierten Pflanzen wurde der Doppelstrangbruch über eine transiente Expression von gRNA und Cas9 induziert, was aus der fehlenden Nachweisbarkeit der entsprechende T-DNA geschlossen wurde. Die nachgewiesenen Mutationen waren erwartungsgemäß heterozygot und/oder chimär. Die Anwesenheit von zwei oder drei mutierten Allelen resultierte z.T. in spezifischen Phänotypen, die eine Verzweigung der Ähre aufwiesen.

Mittels der Analyse von bis zu 5 Generationen von Nachkommen wurden 14 vererbbare Allele für *Branched head* etabliert, davon zwei Mutationen im A-Allel, sieben im B-Allel und fünf im D-Allel. Ein Teil dieser Mutationen führte nicht zur Verschiebung des translationalen Leserahmens, allerdings wird die Funktionalität der AP2-Domäne auch in diesen Fällen beeinflusst. Die mutierten Allele bilden 18 vererbbare Allelkombinationen, welche in keinem Fall zum vollständigen BH-Funktionsverlust führen. Des Weiteren kamen auch zwei nicht vererbbare Allelkombinationen vor, die zu ausbleibendem Kornansatz führten.

Tabelle 1: Übersicht über die Kombinationen mutierter Allele von *Branched head*

Allelkombination	*Bh*-A	*Bh*-B	*Bh*-D	T-DNA
ABD (Bobwhite)	WT	WT	WT	
aBD	Δ1 bp	WT	WT	
	Δ20 bp	WT	WT	
AbD	WT	+1 bp	WT	
	WT	Δ11 bp	WT	
Ab*D	WT	Δ10/+13 bp [2]	WT	
	WT	Δ6 bp [2]	WT	
ABd	WT	WT	Δ11/+1 bp	
	WT	WT	Δ18/+7 bp	
abD	Δ1 bp	+1 bp	WT	
ab*D	Δ20 bp	Δ6 bp [2]	WT	
Abd	WT	+1 bp	Δ11/+1 bp	
Ab*d	WT	Δ39 bp [2]	Δ1 bp	
aBd	Δ1 bp	WT	Δ11/+1 bp	
	Δ1 bp	WT	Δ18/+7 bp	
aBd*	Δ20 bp	WT	Δ15 bp [2]	
abd [1]	+1 bp	Δ5/+31 bp	Δ2 bp	gRNA4, *cas9, hpt*
ab*d [1]	Δ14 bp	Δ24 bp [2]	Δ1 bp	gRNA4, *cas9, hpt*
abd*	Δ1 bp	Δ5/+31 bp	Δ8/+2 bp [2]	gRNA4, *cas9, hpt*
ab*d* bΔ6	Δ20 bp	Δ6 bp [2]	Δ15 bp [2]	gRNA4, *cas9, hpt*
ab*d* bΔ36	Δ20 bp	Δ36 bp [2]	Δ15 bp [2]	gRNA4, *cas9, hpt*

[1] Keine Kornbildung beobachtet [2] Mutation bei verbleibendem Leserahmen (*)

In Pflanzen mit zwei oder drei mutierten Allelen wurden zumeist überzählige Ährchen und Ährenverzweigungen beobachtet (Abbildung 1A, B), wodurch theoretisch das Potential zur Erhöhung der Kornzahl gegeben ist. Letztere war jedoch aufgrund reduzierter Fertilität tendenziell geringer, wohingegen die gebildeten Körner eher breiter und stärker gefüllt waren, was sich in einer erhöhten Tausendkornmasse widerspiegelte (Abbildung 1A). In den meisten Mutationskombinationen war ein geringerer Kornertrag zu beobachten, während die Allelkombinationen ab*D, aBd und aBd* ein gewisses Potential zu erhöhtem Ertrag zeigen (Abbildung 1C). Des Weiteren wurde beobachtet, dass der Funktionsverlust der *Bh*-A-Kopie zu stärker verzweigten und längeren Wurzeln führte (Abbildung 1D). Der vollständige Funktionsverlust von BH bewirkt hingegen eine Missbildung der Ährchen- und Blütchenmeristeme, wodurch eine Kornbildung nahezu ausgeschlossen ist (Abbildung 1E).

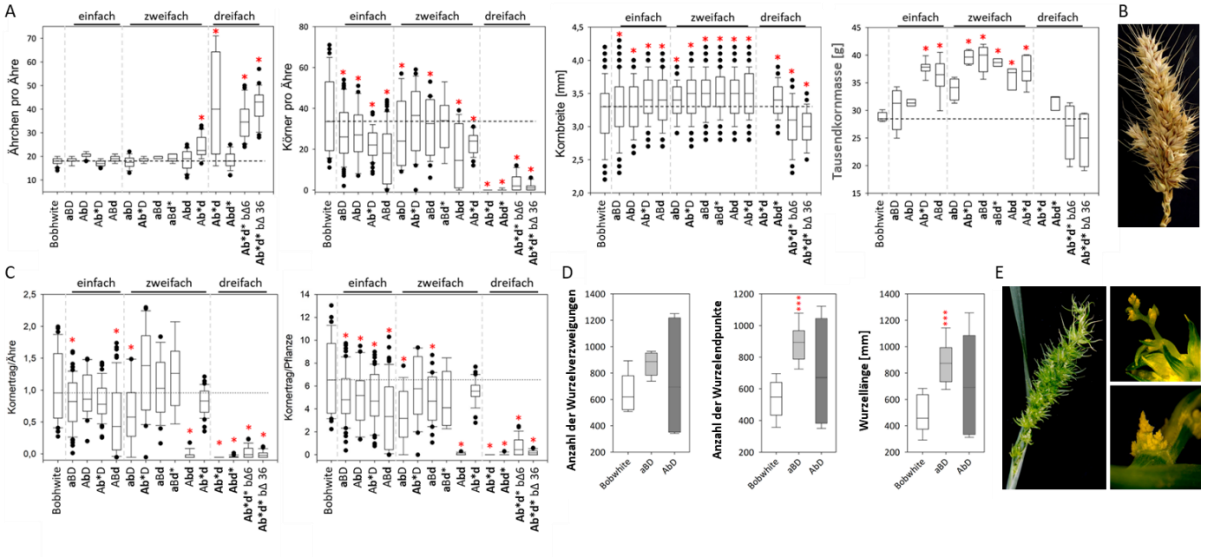

Abbildung 1: Phänotypische Konsequenzen von Mutationen in den *Bh*-Allelen; A) Analyse ertragsrelevanter Parameter (Ährchenzahl und Kornzahl pro Pflanze, Kornbreite, Tausendkornmasse) in Pflanzen mit verschiedenen *Bh*-Allelkombinationen; B) Überzählige Ährchen und Ährenverzweigungen in *bh*-Mehrfachmutante; C) Kornertrag pro Ähre und Pflanze in *bh*-Mutanten; D) Einfluss des Funktionsverlustes des *bh*-A- bzw. B-Homoeoallels auf das Wurzelwachstum; E) Phänotyp bei vollständigem Funktionsverlust von BH; rote Asteriske repräsentieren signifikante Unterschiede zur Wildtyp-Linie Bobwhite; gestrichelte Linie repräsentiert Wildtyp-Median

Zusammenfassung

Die durchgeführten Arbeiten zeigen die funktionelle Bedeutung des Transkriptionsfaktors BRANCHED HEAD, bei dessen Funktionsverlust einerseits mehr Ährchen gebildet werden und Verzweigungen auftreten können, wobei die drei vorhandenen *Bh*-Homoeoallele unterschiedliche quantitative Wirkung aufweisen. Der (partielle) Funktionsverlust der A- und B bzw. A- und D-Kopie birgt ein Potential zur Ertragssteigerung. Um eine züchterische Verbesserung zu erreichen wäre es wünschenswert, weitere Allelvarianten zu generieren und ausgewählte Allelkombinationen in Freilandversuchen testen zu können.

Danksagung

Ich bedanke mich herzlich bei Dr. Jochen Kumlehn für die fachliche und experimentelle Betreuung während meiner Doktorzeit sowie bei meinem Hochschulbetreuer Prof. Dr. Jens Boch und meinen beiden Mentoren Prof. Dr. Thorsten Schnurbusch und Dr. Johannes Thiel für all ihre wertvollen Ratschläge. Großer Dank geht an die technischen Assistentinnen Cornelia Marthe, Carola Bollmann, Ingrid Otto und Nicole Schäfer für ihre erstklassige Hilfe, das Team um Dr. Astrid Junker für die Betreuung bei der Wurzelanalyse sowie den Gärtnern für die Anzucht und Pflege der Pflanzen.

Darüber hinaus gebührt mein Dank dem BMBF und dem PTJ sowie dem Wirtschaftspartner Strube Research GmbH & Co. KG für die Förderung und Unterstützung dieser Arbeiten des OSIRIS-Projektes im Rahmen des Förderprogramms PLANT2030.

Literatur

Dobrovolskaya O, Pont C, Sibout R, Martinek P, Badaeva E, Murat F, Chosson A, Watanabe N, Prat E, Gautier N, Gautier V, Poncet C, Orlov YL, Krasnikov AA, Berges H, Salina E, Laikova L, Salse J (2015) FRIZZY PANICLE drives supernumerary spikelets in bread wheat. Plant Physiol 167:189-199

FAOSTAT Statistical (2019) Food and agriculture organization of the United Nations (FAO). Online, 29 Jun 2021, http://www.fao.org/faostat/en/

Hertig C (2023) Beeinflussung des Ertragspotentials von Gerste und Weizen durch Modifikation ährenarchitektonischer Eigenschaften mittels Cas-Endonuklease-vermittelter Mutagenese. Hannover: Gottfried Wilhelm Leibniz Universität, Dissertation, XX, 217 Seiten, DOI: https://doi.org/10.15488/13269

Ismagul A, Iskakova G, Harris JC, Eliby S (2014) Biolistic Transformation of Wheat withCentrophenoxine as a Synthetic Auxin. In D. Fleury and R. Whitfordt (eds), Crop Breeding. Methods in Molecular biology (Methods and Protocols) Humana Press: New York, NY

Li Y, Li L, Zhao M, Guo L, Guo X, Zhao D, Batool A, Dong B, Xu H, Cui S, Zhang A, Fu X, Li J, Jing R, Liu X (2021) Wheat FRIZZY PANICLE activates VERNALIZATION1-A and HOMEOBOX4-A to regulate spike development in wheat. Plant Biotechnol J, 19: 1141-1154

Narisetti N, Henke M, Seiler C, Shi R, Junker A, Altmann T, Gladilin E (2019) Semi-automated Root Image Analysis (saRIA). Sci Rep 9: 19674

Poursarebani N, Seidensticker T, Koppolu R, Trautewig C, Gawronski P, Bini F, Govind G, Rutten T, Sakuma S, Tagiri A, Wolde GM, et al (2015) The Genetic Basis of Composite Spike Form in Barley and Miracle-Wheat. Genetics 201: 155-165

Ray DK, Mueller ND, West PC, Foley JA (2013) Yield Trends Are Insufficient to Double Global Crop Production by 2050. PLoS One 8: e66428

Vorträge für Pflanzenzüchtung 89, 17-21, 2023

MAPPING AND CHARACTERIZATION OF NEW RESISTANCE TO DOWNY MILDEW IN AN UNEXPLOITED EAST ASIAN VITIS SPECIES

Nagarjun Malagol
Julius Kühn-Institut (JKI), Institute for Grapevine Breeding Geilweilerhof,
76833, Siebeldingen, Germany

Introduction

Grapevine (*Vitis vinifera* L. subsp. *sativa* DC./Hegi) is one of the most widely cultivated and extensively used *Vitis* species in the global wine industry. Concurrently, the grapevine is highly vulnerable to many fungal pathogens resulting in inevitable catastrophic yield losses (Toffolatti et al., 2018). Downy mildew caused by an obligate biotrophic oomycete *Plasmopara viticola* [(Berk. & Curt.) Berl. & de Toni] is one of the most destructive diseases that affect grapevines in warm and humid conditions (Koledenkova et al., 2022). The extensive use of copper-based or synthetic fungicides is imperative to avoid serious yield losses. However, this leads to impact on human health, the environment and decreases in social acceptance (Karimi et al., 2021). Cultivars exhibiting natural resistance serve as one of the potential solutions to downy mildew due to their contribution towards environmentally friendly viticulture (Töpfer & Trapp, 2022). Hence, introducing and pyramiding these naturally occurring resistances of wild *Vitis* species into *V. vinifera* genetic background is an important long-term objective of grapevine breeding (Töpfer et al., 2015). One of the most crucial requirements of plant breeding and genetic mapping programmes is the high-throughput, objective and standardised study of phenotypic evaluation (Tugrul et al., 2022). To date, manual rating has always been the primary method for determining the severity of infestations (Schwander et al., 2012). This task is tedious, time-consuming, subjective and thus prone to errors. The primary objective of this research was therefore to develop an artificial intelligence (AI) based systems to quantify the severity of downy disease as well as leaf hairiness (trichome). The secondary objective was to genetically map and identify a downy mildew resistance in the unexplored East Asian species *V. coignetiae*.

Plant material and phenotyping

As part of the resistance mapping study, a segregating biparental population based on the East Asian *V.* coignetiae called ‘Gf.2018-063’ (‘Morio Muskat’ x COxGT2 (*Vitis coignetiae* x Gewürztraminer), n=496) was utilized (abbreviated: MMx(COxGT2)). For the development of an AI-based downy mildew and leaf hair quantification model, ‘Gf.2018-074’ (Cabernet Dorsa' ('Blaufränkisch' x 'Dornfelder') x Couderc 13 (*Vitis aestivalis* var. lincecumii x Couderc 162-5), n=314) population (abbreviated:

CDxC13) was utilized in addition to the population ‘Gf.2018-063’. The degree of resistance to *P. viticola* phenotypic assessment was performed by artificially inoculated leaf discs. The leaf discs excised were placed upside-down on the 1 % water agar on 96 sample grids followed by artificial inoculation with *P. viticola* spore suspension. Following five days post-inoculation, automated image (RBG) acquisition of treated leaf discs were acquired.

Convolutional neural network (CNN) model development

All the leaf disc images representing inversed OIV452-1 classes were sorted into five different image classes i.e., class I (resistant) and class V (susceptible), whereas, class III ,V & VII are intermediate classes. To produce labelling images, each leaf disc image was sliced into 506 slices. The slices were categorized into background, leaf and sporangiophores using an image-sorter2 script. The first binary CNN1 model was trained to classify between the background and the leaf. The second binary CNN2 model classified leaf with infection and without infection (Figure 1). The model training files of CNN are available on GitHub (https://github.com/Daniel-Ze/Leaf-disc-scoring/tree/main/scripts). Similar to this, a new ResNet-based leaf hair quantification model was developed to investigate relation between the leaf hair density and *P. viticola* (Malagol et al., 2023 in preparation) .

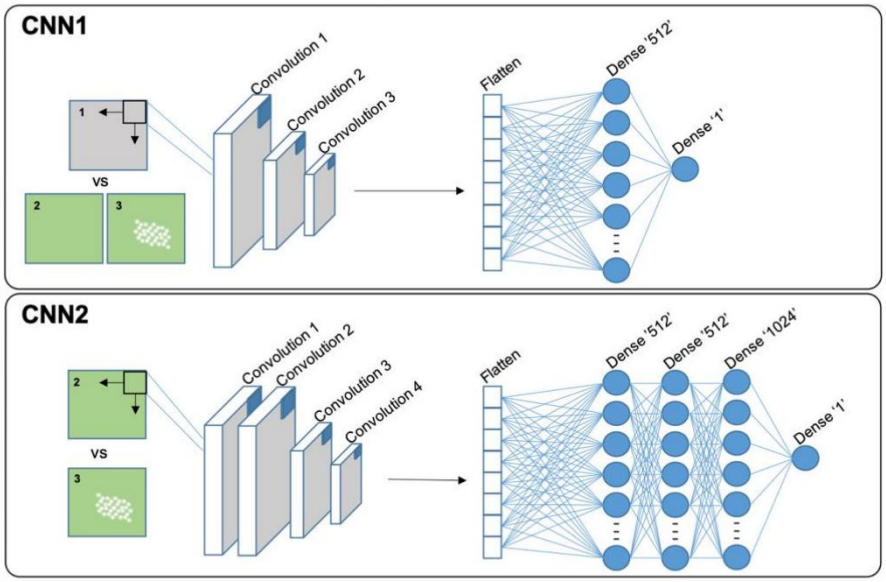

Figure 1: Convolutional architecture of two CNNs. CNN1: background vs. leaf; CNN2= leaf with vs. leaf without infection (Zendler et al., 2021)

Genetic mapping and quantitative trait loci analysis

For marker analysis and creation of a genetic maps, two different DNA marker technologies were implemented i.e., Simple Sequence Repeats (SSR) and rhAmpSeq (RNase H2 enzyme-dependent amplicon sequencing) markers. rhAmpSeq sequenc-

ing was conducted as described in (Zou et al., 2020). The rhAmpSeq-based genetic map was constructed using LepMap3 v. 0.2. QTL analyses were carried out using the R/QTL package (Malagol et al., 2023 in preparation; Malagol, 2023 dissertation, modified).

Results

SCNN training and performance evaluation

The CNN1 (background vs. leaf) achieved an overall model validation accuracy of 98% with a validation loss of 6%. Whereas, the CNN2 (leaf with vs. leaf without infection) achieved a validation accuracy of 95%. A set of two different cross-population (MMx(COxGT2) and CDxC13) images were utilized to test the neural network model performance. Three experts independently generated ground truth for image slices and manual percentage data, which was correlated with the data evaluated by the SCNN. The overall percentage of true positives ranges from ~89-100%. A highly significant correlation of R=0.92 and R=0.91 ($p<0.05$) was observed between the manual scoring and SCNN scorings (%) for the MMx(COxGT2) and CDxC13, respectively. Furthermore, a high correlation of R>0.90 was observed between the OIV classes and SCNN (%) ratings. An example output of the pipeline with the percentage of leaf disc (perc_spo) covered with sporangiophores is shown in the Figure 2.

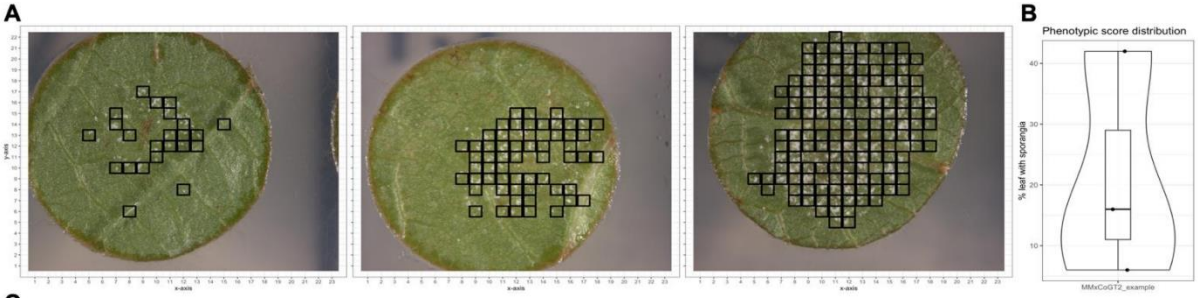

C

Exp_name	Sample	Number	Leaf_disc	Agar	perc_leaf_disc	perc_agar	spo	no_spo	perc_spo	perc_no_spo
MMxCOxGT2	score5_Plate_5_I_s77.jpg	1	362	144	72	28	23	339	6	94
MMxCOxGT2	score7_Plate_4_I_s24.jpg	2	354	152	70	30	58	296	16	84
MMxCOxGT2	score9_Plate_11_II_s30.jpg	3	352	154	70	30	147	205	42	58

Figure 2: Example output of SCNN-based leaf disc scoring pipeline (Zendler et al., 2021).

Quantitative trait loci analysis

Based on 109 SSR markers, a first framework linkage map was generated for the population MMx(COxGT2). The SSR-based genetic map consisted of 19 linkage groups with an average marker density of 5.05 per chromosome. In total, 647 rhAmpSeq haplotype markers were used to generate a map with higher resolution that covered 96% of the physical coverage with an average distance between loci of 3.2 cM. A highly significant and stable QTL for downy mildew resistance was identified on the upper arm of chromosome 14 in the phenotypic evaluation of three differ-

ent years (Figure 3). The QTL detected at a genetic position of 4.5 cM (physical position 6974992 bp) explained the phenotypic trait variance of up to 36.6%.

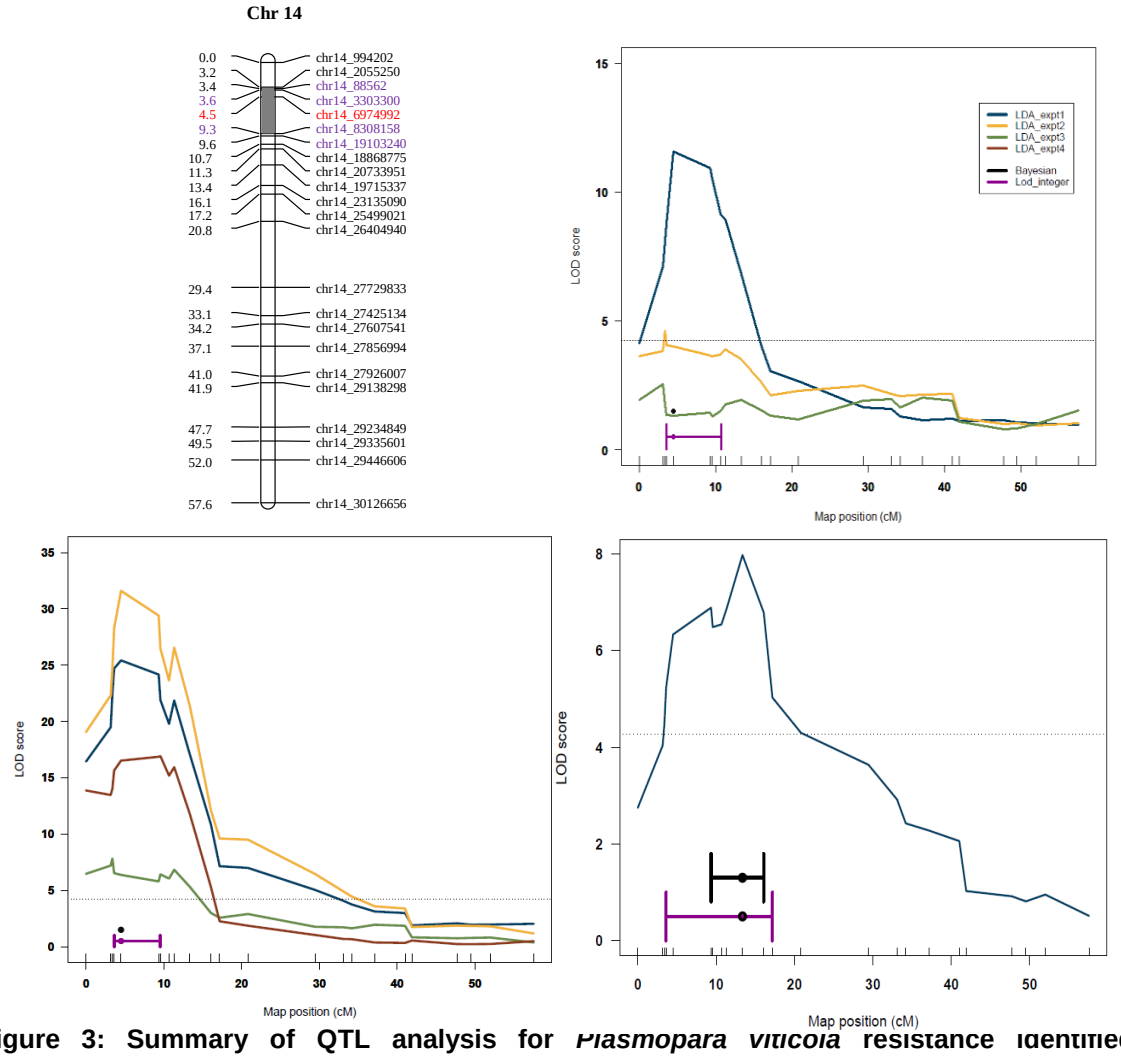

Figure 3: Summary of QTL analysis for *Plasmopara viticola* resistance identified on chromosome 14. (A) Genetic map of chromosome 14 with LODmax marker chr14_6974992 (4.5cM; red) and flanking markers (purple); (B) results of year 2020; (C) 2021; (D) 2022. X-axis indicates map position (cM); Y-axis indicates LOD score. Threshold values are indicated by the dotted line. 'LDA_expt' indicates number of independent leaf Disc Assays each year. (Malagol et al., 2023 in preparation; Malagol, 2023 dissertation, modified).

Conclusion

The SCNN-based novel tool developed in this study is an extremely helpful tool for accurate and high-throughput phenotyping. This pipeline helps in eliminating subjective scoring of the images and use of limited personnel across all experiments. A novel resistance locus for downy mildew resistance located on chromosome 14 in the *V. coignetiae* background has been identified and named as '*Rpv32*'. Potential haplotype marker 'chr14_6974992' linked to the downy mildew resistance can be utilized for marker-assisted selection (MAS) and introgressing '*Rpv32'* into breeding lines, to develop new cultivars with sustainable, environmentally friendly and durable resistance.

Acknowledgements

I am grateful to Prof. Dr. Reinhard Töpfer, Prof. Dr. Rod Snowdon, and Dr. Ludger Hausmann for their excellent supervision. I am thankful to the German Ministry of Food and Agriculture for financing the project VITIFIT under the BLE-BÖL research programme (grant no: 28180E033).

Literature

Karimi, B., Masson, V., Guilland, C., Leroy, E., Pellegrinelli, S., Giboulot, E., & Ranjard, L. (2021). Ecotoxicity of copper input and accumulation for soil biodiversity in vineyards. Environmental Chemistry Letters, 19, 2013-2030.

Koledenkova, K., Esmaeel, Q., Jacquard, C., Nowak, J., Clément, C., & Ait Barka, E. (2022). Plasmopara viticola the Causal Agent of Downy Mildew of Grapevine: From Its Taxonomy to Disease Management. Frontiers in Microbiology, 13, 889472.

Schwander, F., Eibach, R., Fechter, I., Hausmann, L., Zyprian, E., & Töpfer, R. (2012). Rpv10: a new locus from the Asian Vitis gene pool for pyramiding downy mildew resistance loci in grapevine. Theoretical and Applied Genetics, 124(1), 163-176.

Toffolatti, S. L., Russo, G., Campia, P., Bianco, P. A., Borsa, P., Coatti, M. & Sierotzki, H. (2018). A time-course investigation of resistance to the carboxylic acid amide mandipropamid in field populations of Plasmopara viticola treated with anti-resistance strategies. Pest management science, 74(12), 2822-2834.

Töpfer, R., Hausmann, L., Harst, M., Maul, E., Zyprian, E., & Eibach, R. (2011). New horizons for grapevine breeding. Fruit, vegetable and cereal science and biotechnology, 5(1), 79-100.

Töpfer, R., & Trapp, O. (2022). A cool climate perspective on grapevine breeding: climate change and sustainability are driving forces for changing varieties in a traditional market. Theoretical and Applied Genetics, 135(11), 3947-3960.

Tugrul, B., Elfatimi, E., & Eryigit, R. (2022). Convolutional neural networks in detection of plant leaf diseases: A review. Agriculture, 12(8), 1192.

Zendler, D., Malagol, N., Schwandner, A., Töpfer, R., Hausmann, L., & Zyprian, E. (2021). High-throughput phenotyping of leaf discs infected with grapevine downy mildew using shallow convolutional neural networks. Agronomy, 11(9), 1768.

Zou, C., Karn, A., Reisch, B., Nguyen, A., Sun, Y., Bao, Y. & Cadle-Davidson, L. (2020). Haplotyping the Vitis collinear core genome with rhAmpSeq improves marker transferability in a diverse genus. Nature communications, 11(1), 413.

Vorträge für Pflanzenzüchtung 89, 23-27, 2023

"Quantitative effects of the abiotic factors temperature and day length on vernalization, flowering time and freezing tolerance of oilseed rape (Brassica napus L.)."

Eva Heinrich
Department of Crop Sciences, Division of Crop Plant Genetics,
Georg-August Universität, Von-Siebold-Straße 8, 37075 Göttingen

Introduction

Brassica napus L. or oilseed rape is the third largest source of vegetable oil in the world and the most important oil crop in the temperate regions of the earth. Since in oilseed rape the seeds are harvested, the yield for this crop is influenced by seed set and flowering. An important abiotic factor for flowering is day length, which determines the circadian clock, a complex network of genes that change the biochemistry of a plant throughout the day and an important regulator of flowering time (Blümel et al. 2015). *Brassica napus* L. is considered a long-day plant, meaning that a certain minimum day length is required to initiate flowering. Even after the initiation of flowering, a combination of day length and temperature is regulating flowering time by either delaying or accelerating flowering (Blümel et al. 2015).

Temperature is another abiotic factor influencing flowering, growth, and development. Vernalization, a prolonged period of cold initiating flowering, is required in plants with vernalization requirement, like winter oilseed rape. Spring-type rape lacks a vernalization requirement and will be sown in spring, while winter oilseed rape will be autumn-sown and their vernalization requirement prevents preliminary flowering in autumn (Ferreira et al. 1995; Schiessl et al. 2017). Cool temperatures are not only necessary for the fulfillment of the vernalization requirement but also initiate an increase in freezing tolerance to prevent frost damage through a process called hardening (Teutonico and Osborn 1995).

In a nutshell, the abiotic factors temperature and day length influence oilseed rape plant's throughout the year and through a plants whole life cycle, specifically vernalization, flowering time, and freezing tolerance. In this presentation, a doubled haploid (DH) population derived from a cross of a winter and a spring-type oilseed rape was examined for the influence of temperature and day length. The following research questions were asked: (a) How does the vernalization of DH lines influence days to flowering? (b) How do day length and temperature effect the flowering time of fully vernalized plants? (c) Can freezing tolerance be predicted by the phenotype before frost treatment? (d) Is there a connection between the gene networks of freezing tolerance and flowering time regulation?

Materials and methods

The DH-population consisting of 194 lines was derived from a cross between the inbred line 617 of the German winter oilseed rape cultivar ‘Express’ and spring-type doubled haploid line DH4079 derived from the Swedish cultivar ‘Topas’.

The following three sets of replicated experiments were performed: (a) In the vernalization experiment, the plants were grown in the greenhouse in a block design in five replications. Days to flowering (DTF) were recorded on the day of the opening of the first flower. Plants that did not flower after 100 days but showed flower buds were recorded with a value of 115 days and those that did not show flower buds with 130 days. (b) For the day length and temperature experiment, a reduced set of 188 DH lines, the parental genotypes, and the F1 of nine weeks vernalized plants were used. The experiment was a split-split plot design with two factor levels in the main factor temperature (11 and 22°C) and two factor levels in the split factor day length (8 and 16 h) with 5 replications. The experiment was terminated at day 135. Genotypes that did not flower at day 135 but showed buds were recorded with a value of 150 days and if they did not show buds were recorded with a value of 165 days. (c) In the freezing tolerance experiment a reduced set of 184 DH lines was used. The DH lines, the parents and the F1 (200 plants in total) were sown in Styrofoam boxes and hardened for seven weeks at 4 °C and 8 hours artificial light. The experimental design was a simple rectangular lattice design with two sets and was repeated nine times. The plants were scored for several traits four days after the frost treatment (e.g. Stem Damage and Leave Damage scored 1-9), and after a regrowth period (11 days after the end of the frost treatment, e.g. Death as binary). Analysis of variance (ANOVA) was performed with PLABSTAT (Utz 2011). Descriptive statistics, calculation of correlation coefficients and figures were done in R (R. Core Team 2019; Wickham 2016) The linkage marker map consisting of 21,583 SNP markers distributed over 19 linkage groups (Valdés et al. 2018) was used to develop a framework map consisting of 767 markers. QTL mapping and test for epistasis was performed with WinQTL Cartographer software version 2.5 for all experiments (Wang et al. 2012). Candidate genes were searched in the reference genome of rapeseed line ‘Damor-bzh’ (Chalhoub et al. 2014). (d) QTL mapping was examined in a joined analysis.

Results

The vernalization experiment (a) revealed a bimodal distribution of the DH population regarding days to flowering without vernalization. A major QTL for DTF without vernalization (V0a), located on A02 at 42 cM, explained 56% of the phenotypic variance and had an additive effect of 20.2 days. QTL V0a was discovered to have an overlapping confidence interval with QTL for several other flowering time traits. This led to the conclusion that this locus was also a general flowering time loci.

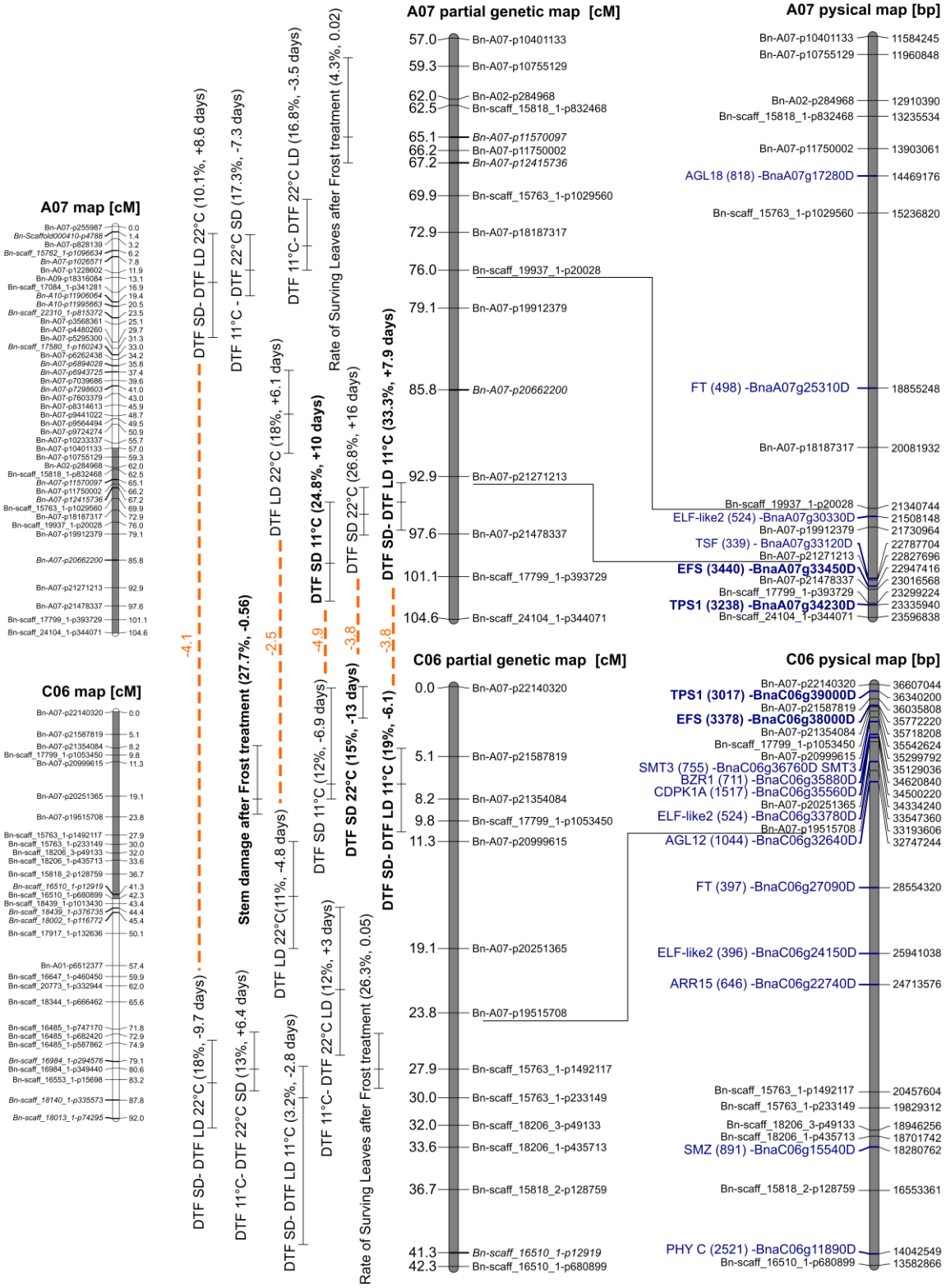

Figure 2: Genetic and physical maps of chromosome A07 (upper half) and C06 (lower half). Left: genetic map of the whole chromosome. Middle: segment of genetic map, marked grey in left map. Selected QTL are given with peak and 95% confidence intervals as well as the variance explained in percent and additive effect in brackets. Epistatic interactions between QTL indicated with dashed line. Right: physical map of segment with candidate genes given with BLAT scores and the respective gene ID in the reference genome of 'Damor-bzh'.

The most likely candidate gene was the well-known flowering time gene FLOWERING LOCUS T (Blümel et al. 2015; Schiessl et al. 2017).

In the day length and temperature experiment (b), the difference in day length between 8 h and 16 h had a large effect on flowering time in this DH population. Short days delay the flowering time. Temperature (11°C and 22°C) alone had a smaller impact than the interaction of temperature and day length. Under short days, a temperature of 22°C led more to a delay of flowering in some DH lines but acceleration in others (with a range of -44 to 40 days), compared to flowering time at 11°C (-20 to 44 days). These two abiotic factors should therefore not be studied independently of each other. On C06, spring-type alleles delayed flowering under short days and at a warm temperature, while on A07, winter-type alleles showed the same effect. For both regions, the candidate gene EARLY FLOWERING IN SHORT DAYS was found. The QTL in these homologous regions had epistatic effects, where the DH4079 alleles on A07 masked the allelic effect on C06 (Figure 1). In the freezing tolerance experiment (c), a novel QTL for freezing tolerance was located on C06 (Figure 1). The joint QTL analysis across experiments (d) revealed that on C06 the major QTL for traits after frost treatment were located in the same region that was a hot spot for flowering time under short days and warm temperatures. Surprisingly, DH lines that did delay flowering under short days were observed to be more sensitive to freezing damage. This is contradictory to the literature, where short days are viewed as signals for the plant to increase freezing tolerance (Jeon and Kim 2013; Roeber et al. 2021).

Summary

In the future, unpredictable winters, warmer spring temperatures, late frost, and other unusual and extreme climate conditions will happen more often due to climate change and pose increased challenges for agriculture, specifically a secure crop production. Here it is shown how the genetic networks of temperature and day length response, as well as vernalization, flowering time regulation, and freezing tolerance are interconnected. Such a genetic diversity and complexity in crops like oilseed rape pose a huge challenge for breeders. But the utilization of different genes as well as gene homologs will also be a chance for plant breeders to combat the emerging challenges of climate change.

Acknowledgments

I thank my thesis commitee: Dr. Christian Möllers, apl. Prof. Dr. Wolfgang Link, and Dr. Antje Schierholt, as well as Dr. Wolfgang Ecke. Thanks to the technical assistants Dietrich Kaufmann, Rosi Clemens and Regina Martsch, and to all the professors, sci-

entists, PhD students and students, and technical personnel/field personnel I was able to meet in this University.

References

Blümel M, Dally N, Jung C (2015) Flowering time regulation in crops—what did we learn from Arabidopsis? Curr. Opin. Biotechnol. 32:121–129. https://doi.org/10.1016/j.copbio.2014.11.023

Chalhoub B, Denoeud F, Liu S, Parkin IAP, Tang H, Wang X, Chiquet J, Belcram H, Tong C, Samans B, Corréa M, Da Silva C, Just J, Falentin C, Koh CS, Le Clainche I, Bernard M, Bento P, Noel B, Labadie K, Alberti A, Charles M, Arnaud D, Guo H, Daviaud C, Alamery S, Jabbari K, Zhao M, Edger PP, Chelaifa H, Tack D, Lassalle G, Mestiri I, Schnel N, Le Paslier M-C, Fan G, Renault V, Bayer PE, Golicz AA, Manoli S, Lee T-H, Thi VHD, Chalabi S, Hu Q, Fan C, Tollenaere R, Lu Y, Battail C, Shen J, Sidebottom CHD, Wang X, Canaguier A, Chauveau A, Bérard A, Deniot G, Guan M, Liu Z, Sun F, Lim YP, Lyons E, Town CD, Bancroft I, Wang X, Meng J, Ma J, Pires JC, King GJ, Brunel D, Delourme R, Renard M, Aury J-M, Adams KL, Batley J, Snowdon RJ, Tost J, Edwards D, Zhou Y, Hua W, Sharpe AG, Paterson AH, Guan C, Wincker P (2014) Plant genetics. Early allopolyploid evolution in the post-Neolithic Brassica napus oilseed genome. Science 345:950–953. https://doi.org/10.1126/science.1253435

Ferreira ME, Satagopan J, Yandell BS, Williams PH, Osborn TC (1995) Mapping loci controlling vernalization requirement and flowering time in Brassica napus. Theor. Appl. Genet. 90:727–732. https://doi.org/10.1007/BF00222140

Jeon J, Kim J (2013) Cold stress signaling networks in Arabidopsis. J. Plant Biol. 56:69–76. https://doi.org/10.1007/s12374-013-0903-y

R. Core Team (2019) R: A Language and Environment for Statistical Computing. https://www.R-project.org/

Roeber VM, Schmülling T, Cortleven A (2021) The Photoperiod: Handling and Causing Stress in Plants. Front Plant Sci 12:781988. https://doi.org/10.3389/fpls.2021.781988

Schiessl S, Huettel B, Kuehn D, Reinhardt R, Snowdon R (2017) Post-polyploidisation morphotype diversification associates with gene copy number variation. Sci Rep 7:41845. https://doi.org/10.1038/srep41845

Teutonico RA, Osborn TC (1995) Mapping loci controlling vernalization requirement in Brassica rapa. Theor. Appl. Genet. 91:1279–1283. https://doi.org/10.1007/BF00220941

Utz HF (2011) PLABSTAT: Ein Computerprogramm zur statistischen Analyse von pflanzenzüchterischen Experimenten. Institute of Plant Breeding, Seed Science and Population Genetics, University of Hohenheim

Valdés A, Clemens R, Möllers C (2018) Mapping of quantitative trait loci for microspore embryogenesis-related traits in the oilseed rape doubled haploid population DH4069 × Express 617. Mol Breeding 38:73. https://doi.org/10.1007/s11032-018-0822-1

Wang S, Basten CJ, Zeng Z-B (2012) Windows QTL Cartographer 2.5, Department of Statistics, North Carolina State University, Raleigh, NC. http://statgen.ncsu.edu/qtlcart/WQTLCart.htm

Wickham H (2016) ggplot2: Elegant Graphics for Data Analysis. Springer-Verlag New York.

Vorträge für Pflanzenzüchtung 89, 29-34, 2023

Investigation of machine learning approaches to predict quantitative traits using environmental and genomic information

Cathy Westhues

Center for Integrated Breeding Research (CiBreed), University of Göttingen, Germany & Division of Plant Breeding Methodology, Department of Crop Sciences, University of Göttingen, Germany.

Current address: Tech Mahindra GmbH, Riesstr. 20, 80992 München, Germany.

Introduction

Adaptation to climate change requires the rapid development of heat- and drought-tolerant plant varieties that exhibit a superior yield stability under unfavorable and uncertain future weather conditions. The expression of complex phenotypic traits, such as grain yield, oil or protein content, depends on multiple quantitative trait loci and on the environmental factors they interact with, resulting in the differential performance of candidate genotypes across environments, algebraically expressed as genotype-by-environment (G×E) interactions. Today, staggering amounts of high-throughput climatic and soil data can be integrated in breeding predictive analytics to predict the potential of genotypes in untested environments (Rogers *et al.* 2022; Jarquín *et al.* 2014). Machine learning (ML) algorithms are especially tailored to take advantage of the extensive phenotypic information acquired over multi-year and multi-location plant breeding trials. Ensemble methods, that combine several weak learners to produce a more robust predictive model, are often very successful in non-linear modeling in large datasets. The main goals of the first two parts of this dissertation were (i) to benchmark ML methods against linear reaction norm models for environment-specific prediction of genotypes' grain yield and plant height to assess the benefit of using ML models with plant breeding datasets; (ii) to develop an R package that facilitates the incorporation of environmental covariates (ECs) and the application of non-linear algorithms for phenotypic prediction. Furthermore, in (iii), the G2F dataset and a wheat dataset were analyzed with reaction norm models using as environmental relationship matrix a nonlinear distance measure named Dynamic Time Warping (DTW), for which the results are not presented here in details.

Material and Methods

In the first part of the thesis (Westhues *et al.* 2021), maize phenotypic data were obtained from the publicly available Genomes to Fields (G2F) Initiative (AlKhalifah *et al.*, 2018; McFarland *et al.*, 2020). Briefly, we retrieved grain yield, plant height and flowering time phenotypic plot data from 2014 to 2017 from a large set of unique

maize hybrids (≈ 2,000), that was produced from various inbred lines and evaluated at various locations across North America. *In silico* genotypes of maize hybrids were constructed based on parental line genotypes, resulting in a final dataset of 107,399 SNPs characterizing 2,033 hybrids. In addition, at each location, weather data were collected from field weather stations. Daily weather data were summarized into a set of weather-based environmental predictor variables to fit the three main developmental stages (vegetative, flowering and grain filling), estimated using the field flowering time data, and included along soil-based (soil texture, organic matter content) environmental covariates (EC) as predictor variables in the prediction models. Overall, this research aimed to predict the performance of these maize hybrids based on their genetic characteristics and on the environmental conditions. Predictive abilities achieved by linear reaction norm models (LRNM) and two machine learning algorithms, Elastic Net and gradient boosted decision trees (GBDT), were compared using different cross-validation (CV) strategies for the two traits grain yield and plant height. These CV strategies mimicked relevant plant breeding problems, for instance prediction of new hybrids in a future year (CV0-Year) or in a new location (CV0-Site). The reaction norm models were defined according to the models proposed by Jarquín *et al.* (2014) and incorporated interactions between SNP markers and ECs using the Hadamard product between a genomic and an environmental relationship matrices. For the ML models, hyperparameters from the GBDT were fine-tuned using Bayesian optimization to prevent overfitting. Finally, feature importances were extracted from the XGBoost model to understand the relative contribution of each predictor variable to the tree-based model.

In the second part, we developed an R package, learnMET (Westhues et al. 2022), that allows to perform ML-based phenotypic predictions using as input data multi-environment trial phenotypic, environmental and genotypic datasets. Various ML methods such as gradient-boosted decision trees, random forests, stacked ensemble models, and multilayer perceptrons are implemented. In addition, these approaches can be assessed for different types of CV schemes particularly relevant in plant breeding. We compared the performance of these models again to reaction norm models using a rice multi-year dataset (Monteverde et al. 2019) and a subset of the dataset G2F. Daily weather data can be automatically retrieved from the NASAPOWER public database or the user can provide data acquired by in-field weather stations that will undergo a data quality procedure.

Results

Within-environment predictive ability for most of the environments was improved when environmental data was added as explanatory variables to the machine learning-based prediction model used to predict grain yield in a new year (Figure 1.A.). For this CV scheme, non-linear GBDT also outperformed all LRNM models. For predic-

tion of yield in a new location, the ML model using only categorical information (year, location IDs) and geographical coordinates yielded better predictive abilities than models integrating quantitative environmental information (Figure 1.B). We noticed that the explicit modeling of G×E interactions in the linear mixed models using the Hadamard product was helpful to enhance predictive abilities, consistent with previous studies (Jarquín *et al.* 2017; de los Campos *et al.* 2020). For plant height, LRNM using solely categorical information reached the best predictive accuracies. Result differences between the two traits are plausible because environmental factors impact yield more than plant height; plant height is characterized by higher heritability. Climatic covariates which are related to heat stress at flowering time, to precipitation frequency and to soil fertility were important to predict grain yield, while soil covariates showed the largest influence on the trait plant height (Figure 2).

In our benchmarking study using learnMET, machine learning models demonstrated competitiveness with the linear reaction norm approach and often outperformed it as the training set size increased. For small training sets, linear models performed better, since the complex ML prediction models might struggle to capture SNP × EC interactions effectively. Machine learning performed particularly well with the G2F data, which had a larger training size and presented a larger environmental variation, making it more relevant for learning G×E patterns compared to the smaller rice dataset.

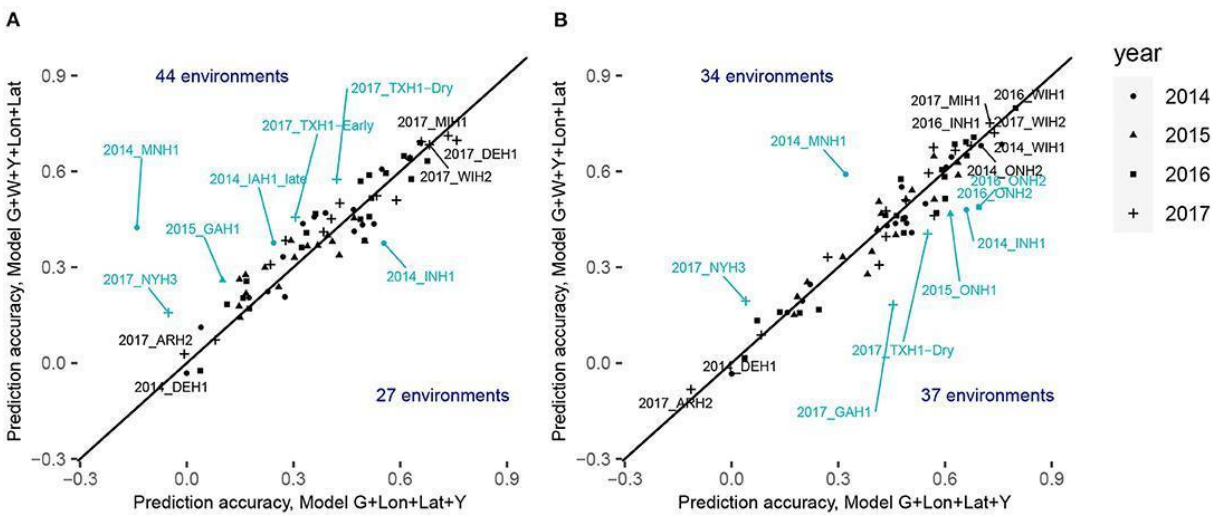

FIGURE 1. Comparison of the within-environment predictive ability with different sets of predictors for the trait grain yield for XGBoost (A) with the CV0-Year scenario and (B) CV0-Site scenario. The x-axis corresponds to the within-environment correlation obtained with the model incorporating PCs derived from SNPs, year and geographical coordinates, while the y-axis corresponds to the correlation obtained with the model that incorporates in addition environmental covariates. Identity (diagonal) line is given. Lighter points with a label indicate environments for which the absolute difference between the two predictive abilities was >0.13.

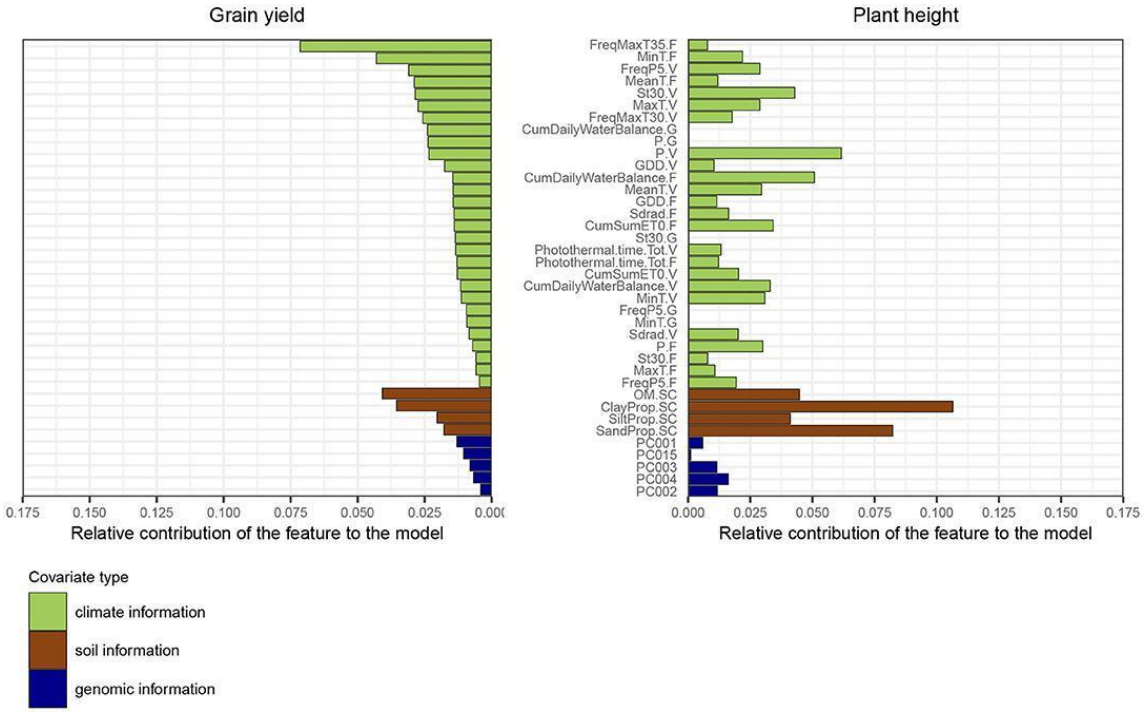

FIGURE 2. Ranking of the importance of features, based on the average relative gain per feature obtained with the model XGBoost that integrated both genomic and environmental data, for the two traits grain yield and plant height. The metric was estimated using a model fitted to the full dataset. The gain represents the improvement in accuracy when using a feature for splitting, across all trees in the model. The sum of all feature contributions is equal to 1. (further details c.f. https://ediss.uni-goettingen.de/handle/11858/14492).

We also demonstrated the importance of expert knowledge (hyperparameter optimization, adequate transformation of the original weather data into stress indices, choice of the algorithm) for an optimal usage of ML methods. Overall, challenges with predictive analytics implying environmental data lie in the difficulty to predict complex traits for observations that fall outside the range of the feature space seen during the training phase. This means that test-set environments that importantly differ from training environments in terms of weather or soil conditions are generally less well predicted in the models that include environmental data. With regard to the analyses conducted with the DTW-based environmental relationship matrix, it was shown that using environmental data was especially advantageous for predicting performance in new environments, and that the explicit inclusion of linear G×E interactions in the models resulted in improved predictive abilities, thus confirming the above mentioned findings.

Conclusions

Our findings emphasize that the use of gradient boosting models resulted in a slight improvement of the within-environment predictive abilities for grain yield in complex prediction scenarios, but no advantage was observed for plant height. Hence, we recommend to carefully consider the heritability of the trait under study that might be

informative about non-additive gene effects and G×E interactions. For grain yield, a trait usually largely influenced by a specific mixture of climatic, soil type and agronomic practices, ML-based methods could provide better predictive abilities than linear random effects. Implementing crop growth models to predict with more precision the plant developmental stages might help improving predictive accuracy in future studies.

Acknowledgments

Financial support was provided by KWS SAAT SE through a Ph.D. fellowship, by the University of Göttingen and by the Center for Integrated Breeding Research. We thank the G2F Consortium for making data publicly available. This work used the High Performance Computing Cluster at GWDG. I also thank my two Ph.D supervisors, Prof. Dr. Timothy Beissinger and Prof. Dr. Henner Simianer, for their great support and advice throughout the thesis. I also acknowledge the relevant comments and advice from Dr. Gregory Mahone and from Dr. Sofia Pereira da Silva.

Literature

AlKhalifah, N., Campbell, D. A., Falcon, C. M., Gardiner, J. M., Miller, N. D., Romay, M. C., ... & Lawrence-Dill, C. J. (2018). Maize genomes to fields: 2014 and 2015 field season genotype, phenotype, environment, and inbred ear image datasets. *BMC research notes*, *11*(1), 1-5.

de Los Campos, G., Pérez-Rodríguez, P., Bogard, M., Gouache, D., & Crossa, J. (2020). A data-driven simulation platform to predict cultivars' performances under uncertain weather conditions. *Nature communications*, *11*(1), 4876.

Hastie, T., Tibshirani, R., and Friedman, J. H. (2009). The Elements of Statistical Learning: Data Mining, Inference, and Prediction. Springer Series in Statistics, 2nd Edn. New York, NY: Springer.

Jarquín, D., Lemes da Silva, C., Gaynor, R. C., Poland, J., Fritz, A., Howard, R., ... & Crossa, J. (2017). Increasing genomic- enabled prediction accuracy by modeling genotype× environment interactions in Kansas wheat. The plant genome, 10(2), plantgenome2016-12.

Jarquín, D., Crossa, J., Lacaze, X., Du Cheyron, P., Daucourt, J., Lorgeou, J., ... & de los Campos, G. (2014). A reaction norm model for genomic selection using high-dimensional genomic and environmental data. *Theoretical and applied genetics*, *127*, 595-607.

McFarland, B. A., AlKhalifah, N., Bohn, M., Bubert, J., Buckler, E. S., Ciampitti, I., ... & De Leon, N. (2020). Maize genomes to fields (G2F): 2014–2017 field seasons: genotype, phenotype, climatic, soil, and inbred ear image datasets. *BMC research notes*, *13*(1), 1-6.

Monteverde, E., Gutierrez, L., Blanco, P., Pérez de Vida, F., Rosas, J. E., Bonnecarrère, V., ... & McCouch, S. (2019). Integrating molecular markers and environmental covariates to interpret genotype by environment interaction in rice (*Oryza sativa* L.) grown in subtropical areas. *G3: Genes, Genomes, Genetics*, *9*(5), 1519-1531.

Rogers, A. R., & Holland, J. B. (2022). Environment-specific genomic prediction ability in maize using environmental covariates depends on environmental similarity to training data. *G3*, *12*(2), jkab440.

Westhues, C. C., Mahone, G. S., da Silva, S., Thorwarth, P., Schmidt, M., Richter, J. C., Simianer, H. & Beissinger, T. M. (2021). Prediction of maize phenotypic traits with genomic and environmental predictors using gradient boosting frameworks. *Frontiers in plant science*, *12*, 699589.

Westhues, C. C., Simianer, H., & Beissinger, T. M. (2022). learnMET: an R package to apply machine learning methods for genomic prediction using multi-environment trial data. *G3*, *12*(11), jkac226.

Vorträge für Pflanzenzüchtung 89, 35-40, 2023

Establishment of maize resistance to fungal diseases by host-induced gene silencing and site-directed mutagenesis

Krishna Mohan Pathi
Julius Kühn-Institut, Institute for Biosafety in Plant Biotechnology,
Erwin-Baur-Straße 27, 06484 Quedlinburg

Introduction

Maize is one of the most cultivated crops in the world. A disease called anthracnose accounts for up to 80% of the loss in maize production. It is caused by the hemibiotrophic fungus *Colletotrichum graminicola*. It also affects vital crops like barley, wheat, and sorghum, often causing over 40% yield reduction, contingent on the crop. (Bergstrom and Nicholson, 1999; Tsror et al., 1999). Unfortunately, the disease is notoriously difficult to combat, since host resistance mechanisms are hardly available (Robertson et al., 2010). In the present investigation, the principle of host-induced gene silencing (HIGS) was employed to protect maize plants from *C. graminicola* infection. HIGS is an RNA-interefence (RNAi)-based process, wherein plant-produced short interfering RNAs (siRNA) are taken up by the fungus and trigger the silencing of cognate genes of the latter (Nowara et al., 2010). In the present study, genes encoding fungicide targets were chosen as HIGS targets, namely *C. graminicola β-Tubulin 2* and *Succinate dehydrogenase 1*.

During the co-evolution, several fungi have taken advantage of using plant genes and derived products for its development and successful colonization. Plant Lipoxygenases (LOXs) are proven for their role in plant-pathogen interaction. Most strikingly, Gao et al. (2007) reported that maize *9-LIPOXYGENASE (LOX3)* acts as a susceptibility factor for *C. graminicola* infections. In addition to the HIGS approach, a further strategy was pursued, which consisted in knocking out a susceptibility factor against *C. graminicola* by means of targeted mutagenesis.

Corn common smut, another important fungal disease, is caused by the biotrophic pathogen *Ustilago maydis*. Intriguingly, transcriptional time-course experiments in *U. maydis*-infected maize revealed a large number of maize genes being upregulated upon the establishment of biotrophy (Doehlemann et al., 2008). Among these genes is the maize *LIPOXYGENASE-3* that has previously been shown to be a susceptibility factor for *C. graminicola* as well. Given this information, maize *LOX3* was chosen to be knocked out, which may provide resistance to both fungal pathogens. Prior to knocking out target gene, it is essential to establish the genome engineering platform in maize. To this end, Cas endonuclease technology was opted, since it was proven to be one of the best available methods to knockout target gene (Kumlehn et al., 2018).

Material and methods

Vectors for RNA-guided Cas9

The highly conserved 5'-untranslated region (UTR) and starting gene segment were utilized for *Cg β-Tub2* (100 nucleotides) and *Cg Sdh1* (117 nucleotides) The fungal 5'-UTR displayed substantial sequence diversity from the host. Selected target sequence were artificially synthesized and cloned into IPKb binary vectors.

Preparation of a *LOX3* knockout construct

The objective was to mutate *LOX3* first exon via targeted mutagenesis. Five motifs in *LOX3* first exon were chosen based on online scores (www.deskgen.com and http://crispr.wustl.edu) and gRNA structures. Corresponding gRNA sequences were inserted between rice u3 promoter and gRNA scaffold, and vector confirmation was done through Sanger sequencing.

gRNA Validation through protoplasts and stable genetic transformation

To validate gRNAs, Cas9 and gRNA components were verified through protoplast transformation. Maize protoplasts were transfected with generated plasmids to confirm functionality. A GFP expression vector was used as a transfection control, following the method outlined by Kmpathi (2021). For the stable transformation studies, Hi-II (A x B) hybrid is used due to its amenability to genetic transformation studies, as described in Hensel Hensel et al. (2009).

C. graminicola Infection and biomass Quantification

Maize leaf segments were inoculated with WT *C. graminicola* strain CgM2 conidia. The inoculated leaves were incubated in the dark at 23°C for up to 120 hours. Fungal DNA quantification was performed using qPCR at 4 days post-inoculation, with Cg-ITS2-qPCR primers specific *to C. graminicola's* rDNA region. External normalization used plasmid pUC18.

U. maydis Infection and biomass Quantification

An experiment assessed resistance of maize *lox3* mutants to *U. maydis* infection. Wild-type strains FB1, FB2, and solo-pathogenic SG200 U. maydis were used. Cultures were prepared and diluted for infection. Syringe infections were made into leaf whorls of 7-day-old maize seedlings. Visual symptoms were categorized over 8 days post-inoculation using a scheme by Kämper et al. (2006). Fungal DNA quantification was conducted on 7-day-old seedlings infected with SG200. Leaf segments were collected at 6 and 12 days post-inoculation, and qPCR using specific primers for the U. maydis Peptidyl-prolyl isomerase (Ppi) gene and maize GAPDH gene was performed for biomass quantification.

Results

HIGS confers quantitative resistance towards *C. graminicola*

Homozygous lines expressing RNAi vectors for two target genes were used to test resistance against *C. graminicola* strain M001. Wild-type azygous Hi-II plants were used as controls. Photographs taken 4 days post-inoculation showed visibly reduced fungal growth in transgenic event 25-2 compared to wild-type. Fungal biomass quantification via DNA content confirmed reduced fungal growth in plant #E-25-2, suggesting host-induced RNAi offers quantitative resistance against *C. graminicola*.

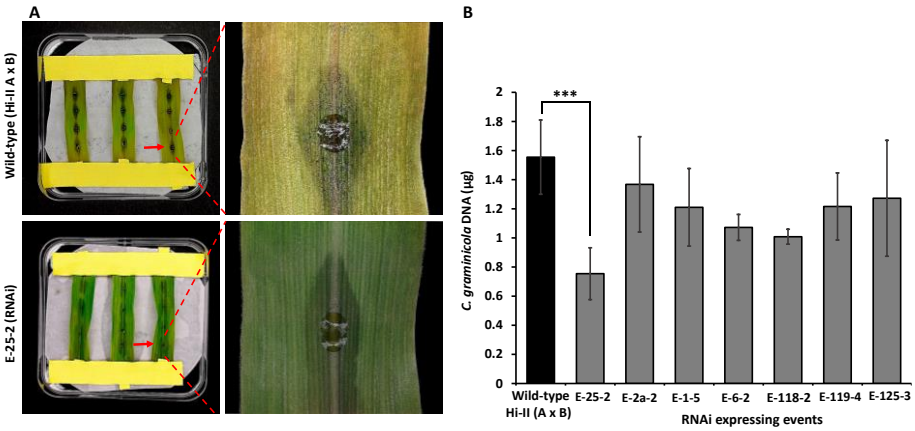

Figure:1 (A) Detached-leaf assay with *C. graminicola* displaying 4-day post-inoculation symptoms. (B) qPCR results using 10 ng DNA template. Columns show means from three independent experiments. Each pool had twelve leaf discs from individual leaves with a single inoculation site. *** denotes significant difference compared to wild-type ($P < 0.001$; one-way ANOVA with Tukey's post-hoc test). Bars represent standard deviation.

lox3 mutants are more resistant to *C. graminicola* than wild-type plants

Homozygous T2 lines of *lox3* mutants with various allelic mutations were infected with *C. graminicola* to assess defense behavior. Drop inoculation caused varying lesion areas in WT and *lox3* mutants. Figure 2A demonstrates the infection severity difference. qPCR-based fungal biomass quantification (Figure 2B) indicated significantly lower fungal levels in *lox3* mutants than wild-type. Allelic mutations of tested mutants are shown in Figure 2C.

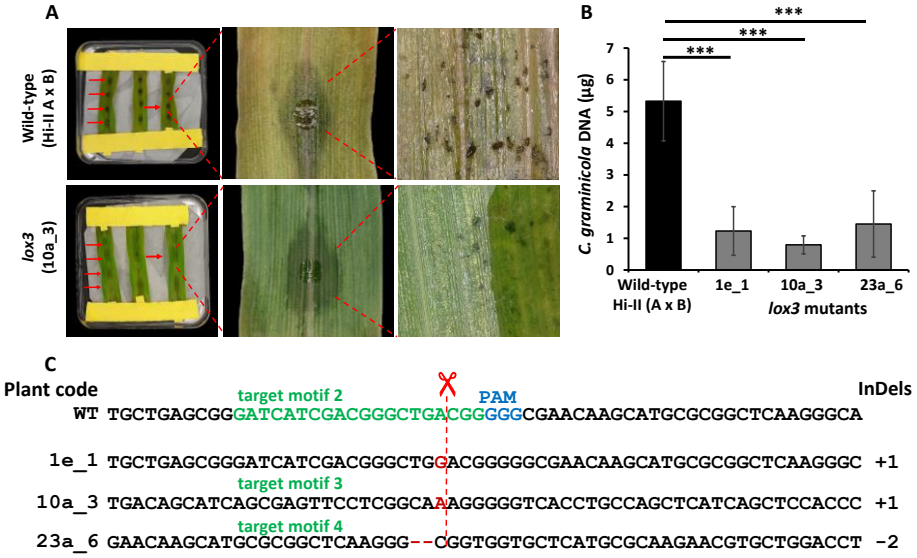

Figure2: Quantitative protection from *C. graminicola* leaf infection of *lox3* mutants

lox3 mutants show moderate resistance to U. maydis infection

Homozygous T2 lines of maize lox3 mutants were tested for *U. maydis* infection susceptibility. Line #13a_8, carrying a 24-nucleotide deletion and a 6-nucleotide insertion, was infected with engineered *U. maydis* SG200. After 8 days, mutants displayed milder symptoms (Figure 30A). Quantification of symptoms (Figure 30B) affirmed mutant resilience. The *lox3* allele of the knockout line is depicted in Figure 30C.

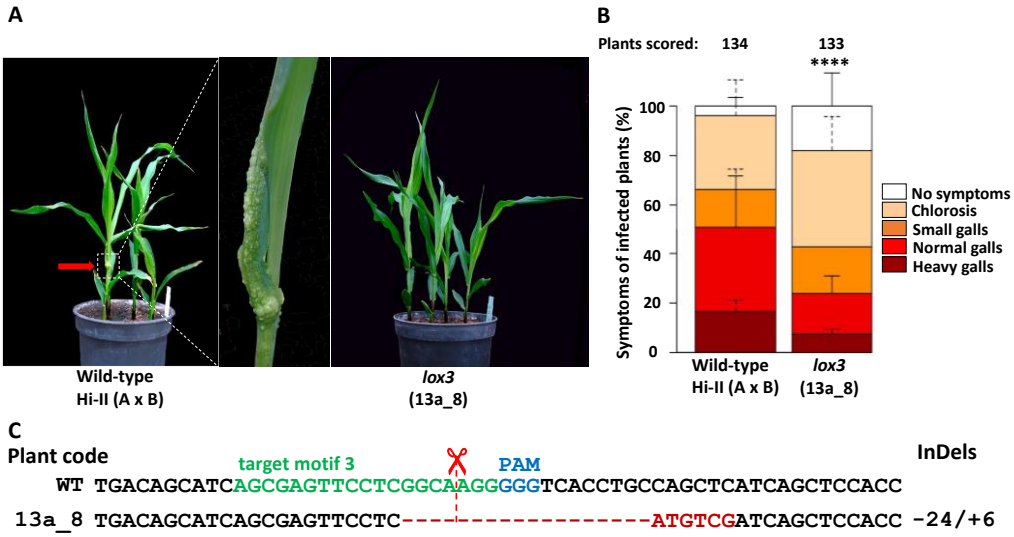

Figure 3: (A) *U. maydis* infection showed heavier gall formation (red arrow) on wild-type compared to *lox3* mutants. (B) Disease rating 8 days post-inoculation (dpi) revealed significant differences between wild-type and mutants (**** p<0.0001). (C) Mutation in *lox3* of the maize line used for assays.

Summary

Transgenic plants expressing RNAi constructs exhibited quantitative resistance against *C. graminicola*. In *C. graminicola* infection assays, homozygous *lox3* mutants displayed reduced fungal colonization and moderate resistance. Similar trends were observed in *U. maydis* infection assays, with *lox3* mutants showing lower disease symptoms and fungal biomass. Notably, increased ROS accumulation in *lox3* mutants, triggered by pathogen-associated molecular patterns (PAMPs), correlated with reduced fungal severity. This study's novel findings suggest that *LOX3* plays a role in susceptibility to *U. maydis*, contributing to a deeper understanding of plant-fungal interactions.

Acknowledgments

I extend my gratitude to Dr. Jochen Kumlehn for his support and guidance during my time in the lab. Prof. Dr. Armin Djamei's valuable guidance in *U. maydis* research is deeply appreciated, as well as the plant reproductive biology group members for their welcoming atmosphere.

Literature

Bergstrom GC, Nicholson RL (1999) The biology of corn anthracnose - Knowledge to exploit for improved management. Plant Disease 83, 596-608

Robertson AE, Pecinovsky K, Liu (2010) Effect of fungicides on anthracnose top dieback, frost severity and yield of hybrid corn at Nashua. Plant Disease Management Reports 4:FC087

Gao XQ, Shim WB, Gobel C, Kunze S, Feussner I, Meeley R, Balint-Kurti P, Kolomiets M (2007) Disruption of a maize 9-lipoxygenase results in increased resistance to fungal pathogens and reduced levels of contamination with mycotoxin fumonisin. Molecular Plant-Microbe Interactions 20, 922-933

Nowara D, Gay A, Lacomme C, Shaw J, Ridout C, Douchkov D, Hensel G, Kumlehn J, Schweizer P (2010) HIGS: host-induced gene silencing in the obligate biotrophic fungal pathogen Blumeria graminis. Plant Cell 22, 3130-3141

Doehlemann G, Wahl R, Horst RJ, Voll LM, Usadel B, Poree F, Stitt M, Pons-Kuhnemann J, Sonnewald U, Kahmann R, Kamper J (2008) Reprogramming a maize plant: transcriptional and metabolic changes induced by the fungal biotroph Ustilago maydis. Plant Journal 56, 181-195

Kumlehn J, Pietralla J, Hensel G, Pacher M, Puchta H (2018) The CRISPR/Cas revolution continues: from efficient gene editing for crop breeding to plant synthetic biology. Journal of Integrative Plant Biology 60, 1127-1153

Pathi K (2021) Establishment of Maize Resistance to Fungal Diseases by Host-induced Gene Silencing and Site-directed Mutagenesis. Doctoral dissertation. Hannover: Institutionelles Repositorium der Leibniz Universität Hannover. xiii, 125 S

Hensel G, Kastner C, Oleszczuk S, Riechen J, Kumlehn J (2009) Agrobacterium-mediated gene transfer to cereal crop plants: current protocols for barley, wheat, triticale, and maize. Int J Plant Genomics 2009, 835608

Kämper J, Kahmann R, Bolker M, Ma LJ, Brefort T, Saville BJ, Banuett F, Kronstad JW, Gold SE, Muller O, Perlin MH, Wosten H.a.B, De Vries R, Ruiz-Herrera J, Reynaga-Pena CG, Snetselaar K, Mccann M, Perez-Martin J, Feldbrugge M, Basse CW, Steinberg G, Ibeas JI, Holloman W, Guzman P, Farman M, Stajich JE, Sentandreu R, Gonzalez-Prieto JM, Kennell JC, Molina L, Schirawski J, Mendoza-Mendoza A, Greilinger D, Munch K, Rossel N, Scherer M, Vranes M, Ladendorf O, Vincon V, Fuchs U, Sandrock B, Meng S, Ho EC.H, Cahill MJ, Boyce KJ, Klose J, Klosterman SJ, Deelstra HJ, Ortiz-Castellanos L, Li WX, Sanchez-Alonso P, Schreier PH, Hauser-Hahn I, Vaupel M, Koopmann E, Friedrich G, Voss H, Schluter T, Margolis J, Platt D, Swimmer C, Gnirke A, Chen F, Vysotskaia V, Mannhaupt G, Guldener U, Munsterkotter M, Haase D, Oesterheld M, Mewes HW, Mauceli EW, Decaprio D, Wade CM, Butler J, Young S, Jaffe DB, Calvo S, Nusbaum C, Galagan J, Birren BW (2006) Insights from the genome of the biotrophic fungal plant pathogen *Ustilago maydis*. Nature 444, 97-101

Vorträge für Pflanzenzüchtung 89, 41-45, 2023

Generierung neuer allelischer Diversität für universelle und dauerhafte Rostresistenz von Weizen und Gerste durch Editierung von SUGAR TRANSPORT PROTEIN 13

Iris Hoffie
Leibniz-Institut für Pflanzengenetik und Kulturpflanzenforschung (IPK),
Corrensstr. 3, 06466 Gatersleben

Einleitung

Pilzkrankheiten wie Braunrost (*Puccinia triticina*), Gelbrost (*Puccinia striiformis*), Schwarzrost (*Puccinia graminis*) und Mehltau (*Blumeria graminis*) stellen eine ständige Bedrohung für die weltweite Getreideproduktion dar. Die sich ändernden klimatischen Bedingungen in den gemäßigten Regionen begünstigen zunehmend die Ausbreitung von Rostpilzen, was zu einem beschleunigten Auftreten neuer Pathotypen und damit verbundener Epidemien führt. Fungizide sind deshalb die am häufigsten eingesetzten Pflanzenschutzmittel in der Getreideproduktion. Doch die wirksamste und umweltfreundlichste Möglichkeit zur Verhinderung dieser Krankheiten ist die Verwendung resistenter Sorten. Die Etablierung breitenwirksamer und dauerhafter Rostresistenz hat ein gewaltiges Potenzial, den Einsatz von Fungiziden im Getreideanbau zu reduzieren. Das Resistenzgen *Lr67* wurde erstmals in Weizen beschrieben und codiert für den Hexose/Protonen-Symporter STP13. Die Resistenz basiert kausal auf einem Basenaustausch im zweiten Exon von *TaSTP13-D*, der den Aminosäureaustausch G144R verursacht (Moore et al. 2015). Das *Lr67res*-Allel des Weizens verleiht eine universelle quantitative Resistenz gegen Braun-, Gelb- und Schwarzrost sowie Mehltau (Herrera-Foessel et al. 2014, Moore et al. 2015). Allerdings konnte dieses Allel aufgrund seiner engen genetischen Kopplung mit dem *REDUCED HEIGHT 1-D* (*RHT1-D*) Wildtypallel bisher nicht für die Züchtung moderner, kurzstrohiger Sorten genutzt werden (Moore et al. 2015). Gerstenlinien mit *TaLr67res*-Transgen erwiesen sich im Vergleich zum Wildtyp ebenfalls als resistent gegen Braunrost und Mehltau (Moore et al. 2015, Milne et al. 2019). Diese Ergebnisse legen nahe, dass das endogene *HvSTP13* ebenfalls ein potenzielles Resistenzgen sein könnte. Um diese Resistenz für die Züchtung aktueller Sorten zu erschließen, wird durch den Einsatz CRISPR-assoziierter (Cas) Endonukleasen eine breite Palette von Gersten- und Weizen-Linien mit *STP13*-spezifisch induzierten Mutationen generiert. Neben dem Versuch die Resistenz-vermittelnde Mutation des *Lr67res*-Allels identisch nachzubilden, sollen dabei auch neue Genvarianten generiert werden, die auf prinzipiell gleiche Weise Resistenz bewirken könnten.

Material und Methoden

Generierung des modularen Vektorsystems CasCADE

Das in dieser Arbeit entwickelte CasCADE-System (Hoffie et al., in Vorbereitung) ist ein vergleichsweise einfaches, aber vielseitiges modulares Vektorsystem für Genom-Editierungsanwendungen mit Fokus auf Getreidepflanzen auf der Grundlage bekannter, gut funktionierender Elemente. Dabei umfasst das Vektorsystem Komponentenkonstellationen für die Genom-Editierung sowohl mono- als auch dikotyler Pflanzenarten. Alle verwendbaren Elemente wie z.B. Promotoren, verschiedene cas9-Derivate und Terminatoren wurden mit Erkennungssequenzen für Typ-IIS-Restriktionsenzyme zur Herausbildung kompatibler Überhänge ausgestattet, so dass mittels Golden-Gate-Klonierungen mehrere Module in nur einer Reaktion zusammengefügt werden können. Zudem können mit CasCADE bis zu vier gRNAs simultan exprimiert werden. Alle Module sind austauschbar, was das CasCADE-System zu einem extrem flexiblen und anpassbaren Werkzeug macht. In insgesamt nur drei Klonierungsschritten lassen sich individuelle gRNA/cas9 Konstrukte für den direkten DNA-Transfer klonieren. Auch die gRNA/cas9-Konstrukte für die gezielte Mutagenese der STP13-Orthologe von Gerste und Weizen wurden mit dem CasCADE-System kloniert.

Pflanzenkultivierung, Transformation und Pflanzenanalyse

Die Gerstenlinie ‚Golden Promise' und die Weizenlinien ‚Bobwhite' und ‚Taifun' dienten als Donormaterial für die Transformationsexperimente. Die Pflanzenanzucht sowie die Agrobakterien-vermittelte Transformation von Weizen- und Gerste erfolgte wie zuvor beschrieben (Marthe et al., 2015). Regenerierte Primärmutanten wurden auf das Vorhandensein des Transgens untersucht und die amplifizierten Zielregionen der M1- und M2-Generation wurden entweder mittels Sanger-Sequenzierung (Gerste) oder Amplikon-Tiefensequenzierung (Weizen) analysiert.

Resistenztests

Drei bis vier Nachkommen der gewählten HvStp13-Mutanten und die Kontrollen ‚Golden Promise' und ‚Großklapprige' wurden mit dem Puccinia hordei-Isolat I-80 im Gewächshaus wie zuvor beschrieben inokuliert (Ivandic et al., 1998; König et al., 2012). Die Symptome wurden 12 Tage nach der Inokulation bonitiert und der Befall anhand einer Skala von 0 (hochresistent) bis 4 (hochanfällig) bewertet (Levine und Cherewick, 1952; Parlevliet, 1976).

Ergebnisse

Zunächst wurde das modulare Vektorsystem CasCADE als generelle Voraussetzung effizienter Genom-Editierung in Getreidepflanzen entwickelt. Mit dessen Hilfe wurden *TaLr67/STP13*- bzw. *HvSTP13*-spezifische gRNA/*cas9*-Konstrukte kloniert. Dabei wurden Zielmotive ausgewählt, die sowohl in der Region des G144R-verursachenden Basenaustausches lokalisiert sind als auch solche, die im ersten und dritten Exon in verschiedenen Transmembran-Domänen liegen, um ggf. auch neuartige Resistenz-vermittelnde Allele gene-

rieren zu können. Stabil-transformierte Weizen- und Gerstenpflanzen wurden generiert und auf Mutationen im *STP13*-Gen analysiert. Insgesamt wurde eine breite Palette neuer *STP13*-Allelvarianten erzeugt, die im Prinzip auf die gleiche Weise wie *Lr67res* Resistenz verleihen könnten. Nach Selbstung dieser primären Mutanten lagen für Gerste transgenfreie und homozygot mutierte Segreganten vor, während in Weizen die meisten Pflanzen in der M_2-Generation noch heterozygot waren. Beispielhaft werden einige der erzeugten Genvarianten in Weizen und Gerste in Abbildung 1A-B dargestellt. Insbesondere wurden Mutanten für weitere Untersuchungen ausgewählt, die keine translationale Leserahmen-Verschiebung (Knock-out) aufweisen und damit das Potential einer verbleibenden, erwartungsgemäß aber deutlich reduzierten Funktionalität des Genproduktes haben. Repräsentativ sind in Abbildung 1C die Proteinsequenzen um die Position 144 für eine Weizen- und eine Gerstenmutante dargestellt. Die Weizenmutante WI10E16-20 hat unter anderem an der Position 144 eine veränderte Aminosäure und der Gerstenmutante BG897E21 fehlt das Resistenz-relevante Glycin144. Mit einigen dieser Gerstenlinien wurden vorläufige Resistenztests durchgeführt, in denen sich nach Inokulation mit Pilzsporen zeigte, dass vier dieser Mutanten weniger anfällig für Braunrost waren. Beispielhaft sind die Ergebnisse der Resistenztest von einer Mutante und dem Wildtyp in Abbildung 1D-E dargestellt. Dabei erwies sich die bereits oben erwähnte *stp13*-Mutante BG897E21 mit dem fehlenden G144 als besonders vielversprechend. Diese und weitere Gersten- und auch Weizen-Linien werden in Zukunft in weiteren Resistenztests umfangreich getestet.

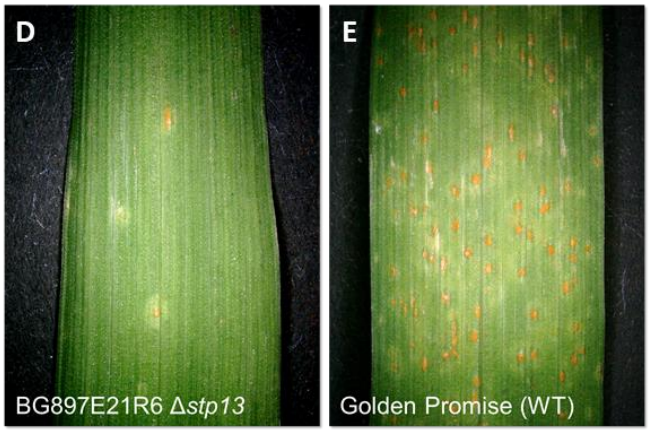

Abbildung 3: Repräsentative, mittels Cas9-vermittelter Mutagenese generierte *STP13*-Allelvarianten von Gerste (A) und Weizen (B). Im Bereich der Zielregionen werden die Proteinsequenzen ausgewählter Mutanten (für Weizen WI10E16-20 und für Gerste BG897E21) dargestellt. Glycin an der Position 144 ist mit roter Schrift gekennzeichnet. Veränderte oder fehlende Aminosäuren sind mit roten Boxen markiert (C). Reduzierte Braunrostanfälligkeit einer *stp13*-Mutante von Gerste (D) im Vergleich zum Wildtyp (E). GP, BW: Wildtyp-Sequenzen der Linien Golden Promise und Bobwhite. TD: Transmembrandomäne

Zusammenfassung

Das im Rahmen dieser Arbeit entwickelte CasCADE-Vektorsystem trägt zu einer erheblichen Verbesserung der Leistungsfähigkeit der Genom-Editierungsplattform des IPK Gatersleben bei. Es findet bereits in über 50 verschiedenen laufenden Projekten inklusive Kooperationen mit zahlreichen internationalen Partnern Anwendung und war Voraussetzung für die Durchführung von mehreren bereits publizierten Studien. Die *Lr67*-vermittelte Resistenz basiert kausal auf einem Basenaustausch im zweiten Exon des Zuckertransporter-Gens *TaSTP13-D*, der den Aminosäureaustausch G144R verursacht. Um diese Resistenz weiter zu erforschen und für die Züchtung aktueller Sorten zu erschließen, wurden in dieser Arbeit mittels Cas9-basierter Genom-Editierung eine breite Palette von Weizen- und Gerstenpflanzen mit

Lr67/STP13-spezifisch induzierten Mutationen generiert. Hierbei lag der Fokus auf der Erzeugung neuer Genvarianten, die auf prinzipiell gleiche Weise Resistenz bewirken könnten. Die daraus resultierenden Mutationen führten zu verschiedenen Veränderungen der Lr67/STP13-Proteinstruktur und erste Resistenztests mit ausgewählten Gerstenmutanten haben ergeben, dass vier der Mutantenlinien potentiell resistent gegen Braunrost sind. Die Weiterführung dieser vielversprechenden Arbeiten erfolgt in einem im April 2023 begonnen, vom BMEL geförderten Projekt.

Danksagung

Ich danke Dr. Dragan Perovic, Dr. Albrecht Serfling und ihren Arbeitsgruppen am Julius Kühn-Institut in Quedlinburg für die Durchführung der Resistenztests. Mein besonderer Dank gilt Cornelia Marthe, Sybille Freist und Sabine Sommerfeld für ihre hervorragende Unterstützung bei der Transformation von Weizen und Gerste.

Literatur

Herrera-Foessel, S.A., Singh, R.P., Lillemo, M., Huerta-Espino, J., Bhavani, S., Singh, S., Lan, C., Calvo-Salazar, V., and Lagudah, E.S. (2014). Lr67/Yr46 confers adult plant resistance to stem rust and powdery mildew in wheat. Theoretical and Applied Genetics 127, 781–789.

Ivandic, V., Walther, U., and Graner, A. (1998). Molecular mapping of a new gene in wild barley conferring complete resistance to leaf rust (Puccinia hordei Otth). Theoretical and Applied Genetics 97, 1235–1239.

König, J., Kopahnke, D., Steffenson, B.J., Przulj, N., Romeis, T., Röder, M.S., Ordon, F., and Perovic, D. (2012). Genetic mapping of a leaf rust resistance gene in the former Yugoslavian barley landrace MBR1012. Molecular Breeding 30, 1253–1264.

Levine, M.N., and Cherewick, W.J. (1952). Studies on dwarf leaf rust of barley. Technical Bulletins 156508.

Marthe, C., Kumlehn, J., and Hensel, G. (2015). Barley (Hordeum vulgare L.) transformation using immature embryos. Methods in Molecular Biology 1223, 71–83.

Milne, R.J., Dibley, K.E., Schnippenkoetter, W., Mascher, M., Lui, A.C.W., Wang, L., Lo, C., Ashton, A.R., Ryan, P.R., and Lagudah, E.S. (2019). The wheat Lr67 gene from the Sugar Transport Protein 13 family confers multipathogen resistance in barley. Plant Physiology 179, 1285–1297.

Moore, J.W., Herrera-Foessel, S., Lan, C., Schnippenkoetter, W., Ayliffe, M., Huerta-Espino, J., Lillemo, M., Viccars, L., Milne, R., Periyannan, S., Kong, X., Spielmeyer, W., Talbot, M., Bariana, H., Patrick, J.W., Dodds, P., Singh, R., and Lagudah, E. (2015). A recently evolved hexose transporter variant confers resistance to multiple pathogens in wheat. Nature Genetics 47, 1494–1498.

Parlevliet, J.E. (1976). The genetics of seedling resistance to leaf rust, Puccinia hordei Otth. in some spring barley cultivars. Euphytica 25, 249–254.

Vorträge für Pflanzenzüchtung 89, 47-52, 2023

Breeding for Improved Flavour of Fresh Market Tomatoes: Breeders' Sensory Test and Molecular Markers

Julia Hagenguth
Georg-August-Universität Göttingen, Division of Plant Breeding Methodology,
Carl-Sprengel-Weg 1, 37075 Göttingen

Introduction

Despite the general popularity of tomatoes, consumers are often dissatisfied with the flavour of fresh market tomatoes (Causse et al., 2003). Flavour is defined as a complex interaction of taste (sugars, acids) and aroma (volatile compounds) (Tikunov et al., 2020). This chemical complexity makes it difficult to assess flavour, especially for hundreds of small samples typical of early breeding generations. Human sensory panels are the most appropriate method to characterize flavour, but are not suitable for large numbers of samples (Colantonio et al., 2022). Simple physicochemical measurements such as total soluble solids (TSS) and titratable acidity (TA) can be used to approximate taste, but not aroma (Causse et al., 2003). Small sensory panels of one to a few persons are probably a common practice in plant breeding programs (Colantonio et al., 2022; Horneburg et al., 2009), but are less evaluated and not standardized. Marker-assisted selection (MAS) is an interesting alternative to phenotypic selection (Causse et al., 2003). However, sensory attributes have rarely been investigated in mapping studies of tomato (Tikunov et al., 2020). Verification of QTL in multiple genetic backgrounds is hardly done (Chaïb et al., 2006).

Materials and Methods

The first study was based on 32 crosses whose parental cultivars were selected based on quality traits and yield from a previous study (Chea et al., 2021; Erika et al., 2022). All three trials (Figure 1) were conducted in organic low-input (Reinshof experimental station, University of Goettingen) and hydroponic (Department of Horticultural Production, University of Applied Sciences Osnabrueck) cultivation. In the first study, ten F_2 plants from each cross and the corresponding parents (in total 910 individuals) were characterized for sensory attributes, physicochemical measurements, aroma volatiles and fruit weight. Perceived sweetness, sourness and tomato aroma were assessed using the Breeders' Sensory Test, a sensory method developed to evaluate hundreds of small samples (Hagenguth et al., 2022). In the second study, one of the crosses, Resi × Auriga, was chosen as F_2 mapping population. Both open-pollinated cultivars had been characterized by superior but contrasting fruit quality and very different fruit weight. In each cultivation system, 190 individuals of the F_2 mapping population were grown with two replications. To map QTL for flavour-related

traits, including sensory attributes, plants were genotyped with the Axiom 200K SOLCUC vegetable array and phenotyped for the same traits as in the previous year.

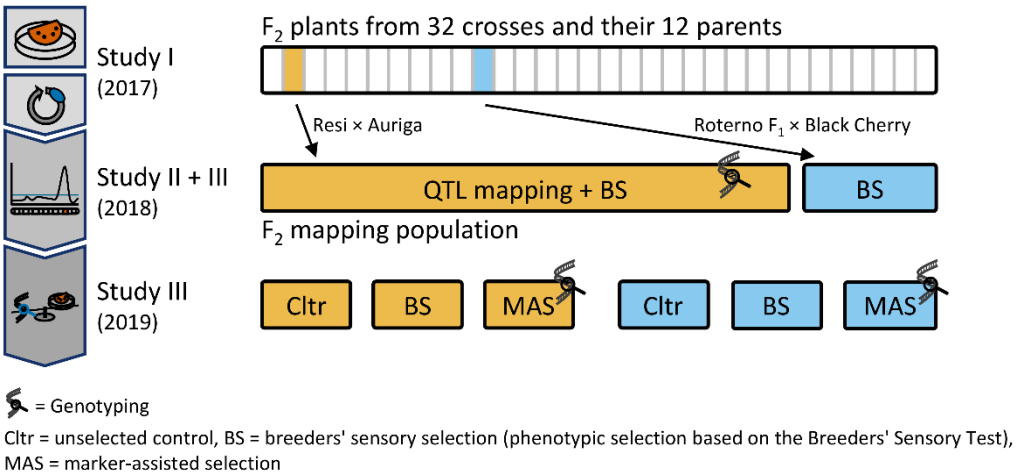

Figure 2: Plant material used in three trials conducted in organic low-input and hydroponic cultivation

For the third study, phenotypic selection based on the Breeders' Sensory Test (breeders' sensory selection, BS) was performed on F_2 plants of the mapping population and the unrelated cross Roterno F_1 × Black Cherry. Roterno F_1 is a high yielding hybrid and Black Cherry an open-pollinated cultivar with excellent sensory attributes. Based on the results of the mapping study, five QTL for the sensory attributes sweetness, sourness and tomato aroma were selected for verification in two genetic backgrounds. In both crosses, MAS was performed on F_2 seedlings. Subsequently, F_3 progenies of plants selected by BS and F_2 plants selected by MAS and an unselected F_2 population were phenotyped.

Results

For the diverse set of genotypes, highly significant correlations between corresponding sensory attributes and physicochemical measurements, namely sweetness and TSS as well as sourness and TA, were observed. The genetic plus environmental variance (coefficient of variation of the F_2 plants) exceeded the environmental variance (mean of the parental coefficients of variation) for most flavour-related traits of most crosses in both cultivation systems (Figure 2). Thus, selection between individual plants is expected to be successful.

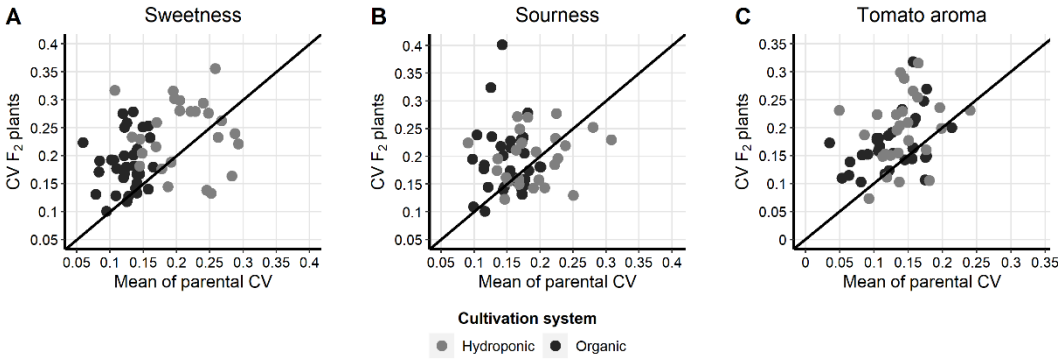

Figure 2: Coefficient of variation (CV) of F_2 plants ($n_{hydroponic}$ = 26, $n_{organic}$ = 32) and the mean CV of the respective parents for (A) sweetness, (B) sourness and (C) tomato aroma

Based on multiple-QTL mapping, a total of 71 QTL was detected for the mean values of both cultivation systems, 61 QTL for organic and 46 QTL for hydroponic cultivation. A proportion of 27% of the QTL was co-localized between both cultivation systems and their mean values, representing robust QTL. QTL for sensory attributes on chromosomes 5 and 10 provide novel information. Nine QTL clusters were identified for the mean values of both cultivation systems, comprising co-localized QTL for different trait classes, e.g. sensory attributes and physicochemical measurements or volatiles. Co-localized QTL for fruit weight and flavour-related traits with antagonistic effects were identified.

Compared to the unselected control, increases in the population means by BS and MAS were observed for most sensory attributes in both crosses and cultivation systems (Figure 3). BS significantly increased sweetness of Roterno F_1 × Black Cherry in organic cultivation. In both crosses, MAS was most efficient for tomato aroma. In addition, a significant increase in sweetness by MAS was observed in Roterno F_1 × Black Cherry in the organic cultivation system. For most traits, the population selected by molecular markers showed the highest mean value for both crosses and cultivation systems. Selection for sensory attributes independent of the selection method resulted in indirect effects on the level of some physicochemical measurements and volatile compounds; fruit weight was decreased.

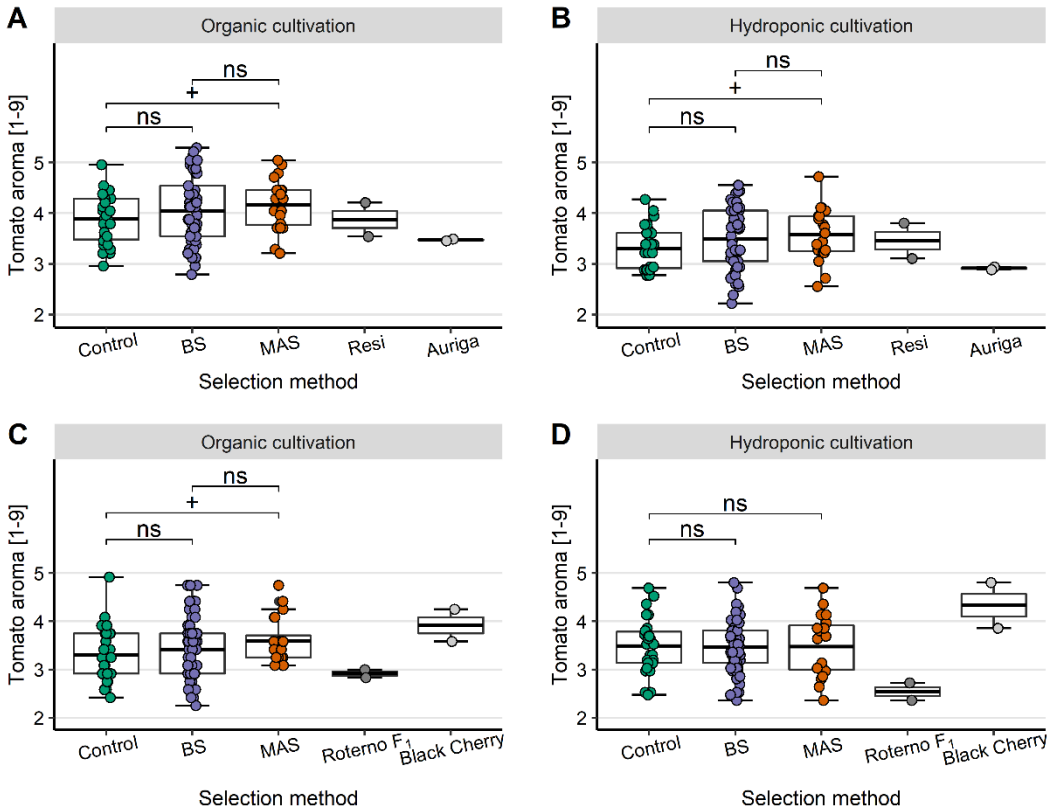

Figure 3: Comparison of breeders' sensory selection (BS) and marker-assisted selection (MAS) with an unselected control for tomato aroma of Resi × Auriga in (A) organic and (B) hydroponic cultivation and Roterno F_1 × Black Cherry in (C) organic and (D) hydroponic cultivation; the bold line represents the mean value; $^{+}$significant at p = 0.1

Conclusions

For sensory attributes, genetic improvement starting with selection in the F_2 generation is expected to be successful. Early selection for sensory attributes using the Breeders' Sensory Test and marker-assisted selection are both promising methods to improve the flavour of tomatoes. Marker-assisted selection is particularly interesting for preselection of seedlings and allows a potentially higher selection intensity, as a very large number of plants can be analysed. Phenotypic selection using the Breeders' Sensory Test accounts for the whole flavour diversity, with mature fruits required. Therefore, to maximize the response to selection and capture all genetic loci including unidentified ones, a combination of both methods is recommended. Our results provide relevant information to improve the flavour of fresh market tomatoes, a trait demanded by consumers. Breeding is the first step in the value chain and improved genetics form the basis for flavourful tomatoes.

Acknowledgments

The PETRA^{q+n} project was financially supported by the Ministry of Science and Culture of Lower Saxony. The Software AG Foundation supported the Section of Genetic Resources and Organic Plant Breeding, University of Goettingen. I received a scholarship from the Professor Werner Schulze-Stiftung zur Förderung der Pflanzenbauwissenschaften for completing my thesis. We thank Dr. Larissa Kanski (Division of Quality of Plant Products, University of Goettingen) for conducting the analytical measurements, Hannah Kahle and Prof. Andreas Ulbrich (Department of Horticultural Production, University of Applied Sciences Osnabrueck) for supervising the trials in hydroponic cultivation. Culinaris – Saatgut für Lebensmittel supported the Breeders' Sensory Test and the organic trials. We acknowledge all people who supported the sensory assessment and all technicians who supported the trials and analyses. I am thankful to my supervisors Prof. Heiko C. Becker and Dr. Bernd Horneburg for all their guidance and advices during my time as PhD candidate.

Refernces

Causse, M., Buret, M., Robini, K., & Verschave, P. (2003). Inheritance of Nutritional and Sensory Quality Traits in Fresh Market Tomato and Relation to Consumer Preferences. Journal of Food Science, 68(7), 2342–2350. https://doi.org/10.1111/j.1365-2621.2003.tb05770.x

Chaïb, J., Lecomte, L., Buret, M., & Causse, M. (2006). Stability over genetic backgrounds, generations and years of quantitative trait locus (QTLs) for organoleptic quality in tomato. Theoretical and Applied Genetics, 112(5), 934–944. https://doi.org/10.1007/s00122-005-0197-7

Chea, L., Erika, C., Naumann, M., Smit, I., Horneburg, B., & Pawelzik, E. (2021). Morphological, Leaf Nutrient, and Fruit Quality Characteristics of Diverse Tomato Cultivars under Organic Low-Input Management. Sustainability, 13(21), 12326. https://doi.org/10.3390/su132112326

Colantonio, V., Ferrão, L. F. V., Tieman, D. M., Bliznyuk, N., Sims, C., Klee, H. J., Munoz, P., & Resende, M. F. R. (2022). Metabolomic selection for enhanced fruit flavor. Proceedings of the National Academy of Sciences, 119(7), e2115865119. https://doi.org/10.1073/pnas.2115865119

Erika, C., Ulrich, D., Naumann, M., Smit, I., Horneburg, B., & Pawelzik, E. (2022). Flavor and Other Quality Traits of Tomato Cultivars Bred for Diverse Production Systems as Revealed in Organic Low-Input Management. Frontiers in Nutrition, 9, 916642. https://doi.org/10.3389/fnut.2022.916642

Hagenguth, J., Kanski, L., Kahle, H., Naumann, M., Pawelzik, E., Becker, H. C., & Horneburg, B. (2022). Breeders' Sensory Test: A new tool for early selection in breeding for tomato (Solanum lycopersicum) flavour. Plant Breeding, 141(1), 96–107. https://doi.org/10.1111/pbr.12994

Horneburg, B., Bauer, D., & Bufler, G. (2009). Züchterische Verbesserung der sensorischen Qualität der Pastinake (Pastinaca sativa L.) im Praxisbetrieb. In J. Mayer, T. Alföldi, F. Lei-

ber, D. Dubois, P. Fried, F. Heckendorn, E. Hillmann, P. Klocke, A. Lüscher, S. Riedel, M. Stolze, F. Strasser, M. van der Heijden, & H. Willer (Eds.), Werte—Wege—Wirkungen: Biolandbau im Spannungsfeld zwischen Ernährungssicherung, Markt und Klimawandel: Vol. Band 1: Boden, Pflanzenbau, Agrartechnik, Umwelt-und Naturschutz, Biolandbau international, Wissensmanagement (pp. 232–235). Verlag Dr. Köster, Berlin, Germany.

Tikunov, Y. M., Roohanitaziani, R., Meijer-Dekens, F., Molthoff, J., Paulo, J., Finkers, R., Capel, I., Carvajal Moreno, F., Maliepaard, C., Nijenhuis-de Vries, M., Labrie, C. W., Verkerke, W., van Heusden, A. W., van Eeuwijk, F., Visser, R. G. F., & Bovy, A. G. (2020). The genetic and functional analysis of flavor in commercial tomato: The FLORAL4 gene underlies a QTL for floral aroma volatiles in tomato fruit. The Plant Journal, 103(3), 1189–1204. https://doi.org/10.1111/tpj.14795

Vorträge für Pflanzenzüchtung 89, 53-57, 2023

Mechanisms of quantitative disease resistance in the maize-Ustilago maydis interaction

Selma Schurack

Julius Kuehn-Institute, Institute for Breeding Research on Agricultural Crops, Robert-Schick-Platz 3a, 18190 Sanitz OT Groß Lüsewitz, Germany

Introduction

In natural environments, plants are constantly exposed to a variety of potentially pathogenic microbes. To protect themselves, they have evolved multiple layers of immune responses and in turn, microbes have developed so-called effectors to cope with or suppress these immune responses.

The biotrophic fungus *Ustilago maydis* causes smut disease on maize (*Zea mays*) and induces the formation of tumours on all aerial parts of the plant (Basse & Steinberg, 2004; Kämper et al., 2006). Unlike in other biotrophic interactions, no gene-for-gene interactions have been identified in the maize-*U. maydis* pathosystem. Thus, maize resistance to *U. maydis* is considered a polygenic, quantitative trait (Hoover, 1932; Immer, 1927). For one *U. maydis* effector, ApB73, a maize line-dependent contribution to virulence has been observed (Stirnberg & Djamei, 2016). This suggests that the fungus' effectors might target certain host genes contributing to quantitative disease resistance (QDR). However, the molecular basis of QDR in maize and how *U. maydis* interferes with its components is still mostly unknown.

Material and Methods

Zea mays L. lines Early Golden Bantam (EGB, Olds Seeds, Madison, WI, USA) and the inbred founder lines of the Nested Association Mapping (NAM) population (Yu et al. 2008; McMullen et al. 2009; North Central Regional Plant Introduction Station, IA, USA) were used for infections. All *U. maydis* strains used in this study were derived from the solopathogenic strain SG200 (Kämper et al. 2006). To generate *U. maydis* knock-out (KO) mutants, the CRISPR-Cas9 system was employed (Schuster et al., 2016).

Results

To investigate quantitative disease resistance in the maize-*U. maydis* interaction, we first evaluated the susceptibility of different maize lines to *U. maydis* infection. Seedlings were inoculated with *U. maydis* SG200 in the greenhouse, and disease symptoms were scored 12 days post inoculation (dpi) according to Redkar & Doehlemann (2016). In this experimental set-up, resistance levels were highly diverse and ranged

from very susceptible to very resistant (>94% vs. <35% tumours, respectively), while no maize line showed complete resistance to *U. maydis* infection (Fig. 1), which further corroborated the quantitative nature of the interaction.

Based on these results, a transcriptome analysis (RNA-Seq) of six *U. maydis*-infected maize lines of highly distinct resistance levels was performed. In accordance with the complex nature of QDR, the different maize lines showed specific responses of diverse cellular processes to *U. maydis* infection. On the fungal side, 406 genes were differentially expressed between maize lines. Strikingly, amongst the 406 differentially expressed genes (DEGs), 102 encode candidate secreted effector proteins (CSEPs, Dutheil et al., 2016) which represents a significant 3.3-fold enrichment (hypergeometric p value 5.65e-30). This indicates an important role of CSEPs in colonising host lines of different resistance levels and in targeting components of QDR.

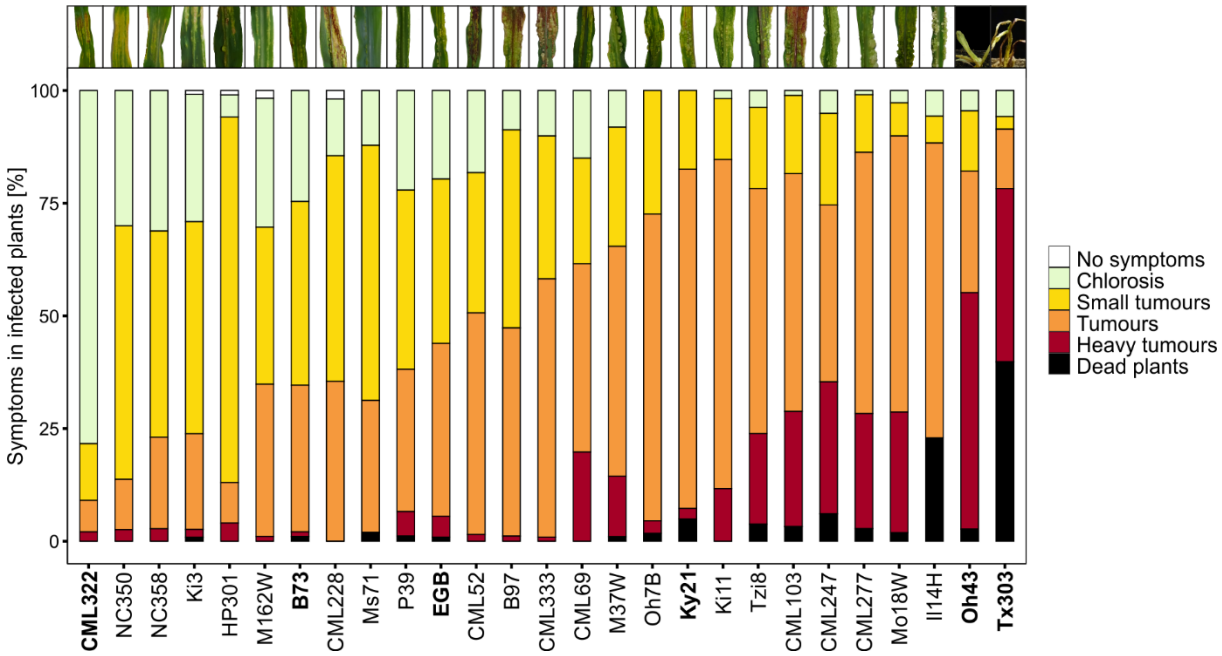

Figure 4: *U. maydis* disease development in the 26 maize NAM founder lines and EGB. Maize seedlings were infected with *U. maydis* SG200 at the three-leaf stage in the greenhouse. Three independent experiments were performed, and the average values are expressed as percentage of the total number of infected plants. Disease symptom classification was done 12 days post infection (dpi) as described in Redkar & Doehlemann (2016). Average number of infected plants per line: 102. Maize lines selected for RNA sequencing are highlighted in bold. Representative pictures of infected leaves at 12 dpi for each maize line are shown at the top.

As *U. maydis* genes encoding CSEPs were enriched in genes differentially expressed between maize lines, we investigated whether line-specifically expressed CSEPs also had line-specific functions for virulence. CSEPs with similar expression patterns were targeted for simultaneous knock-out in the SG200 background (Schuster et al., 2016). Plant infections with the generated *U. maydis* mutant strains

identified line-specific virulence functions for the CSEP genes UMAG_02297 and/or UMAG_05027 (Fig. 2A). While virulence of the double mutant KO_UMAG_02297/KO_UMAG_05027 was not reduced on B73 or EGB, a significant reduction was observed on CML322 and Oh43. To assess if both or only one of the genes contribute to maize line-specific virulence, single KO mutants of UMAG_02297 and UMAG_05027 were tested for virulence on EGB and CML322. This showed that UMAG_02297 alone, but not UMAG_05027, was necessary for full virulence on CML322. The virulence defect of KO_UMAG_02297 could be restored by introducing a single copy of UMAG_02297 into the mutant strain (Fig. 2B).

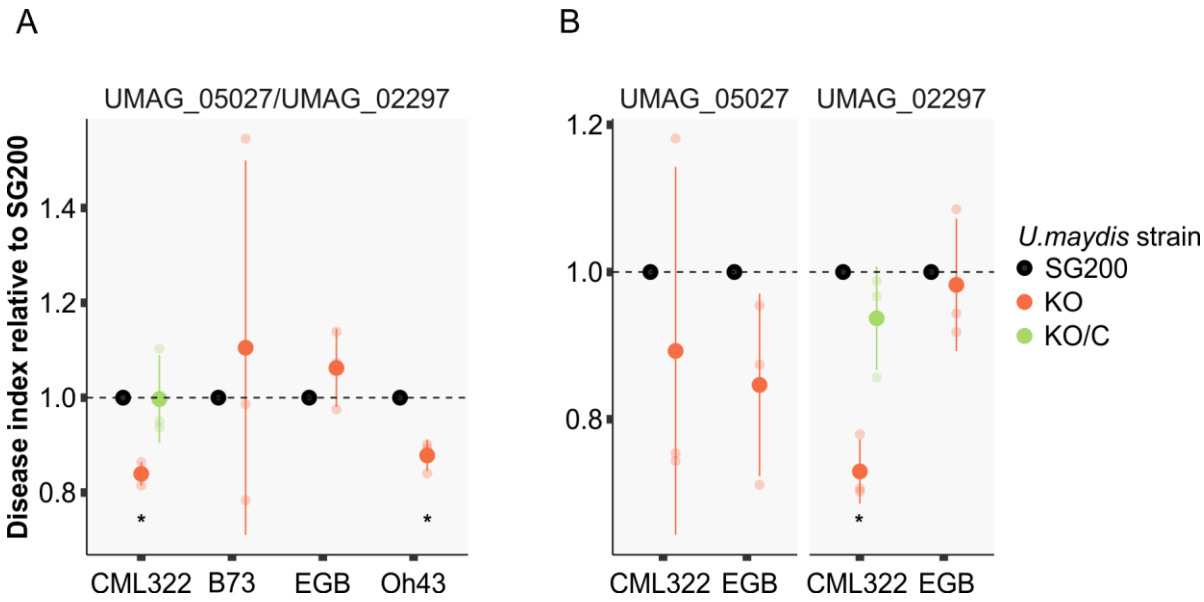

Figure 2: Virulence functions of candidate maize line-specific effectors. Double and single knock-out (KO) mutant strains of selected maize line-specific effectors were injected into maize seedlings of the indicated line and symptoms were scored 12 days post infection (dpi). Gene names are shown at the top. KO refers to the respective CRISPR/Cas9 KO strain. Gene names separated by slash indicate double KO of these genes. KO/C indicates that a single copy of the respective gene was introduced into the KO strain for complementation. Disease indices reflect disease symptom severity and are shown in relation to SG200, which was set to unity. Asterisks label significant reduction in disease index compared to SG200 (student's t-test, p value < 0.05). All experiments were performed in three independent biological replicates. Average number of infected plants per strain and maize line: 89.

To investigate which host processes might be influenced by the maize line-specific effector UMAG_02297, leaf samples of CML322 maize seedlings infected with SG200 and KO_UMAG_02297 were analysed by RNA-Seq. Genes uniquely responsive to each of the strains were additionally filtered for genes that were differentially expressed in response to *U. maydis* SG200 infection between CML322 and EGB, where UMAG_02297 was not found to have a function for virulence (426 genes). Within these, genes predicted to encode auxin efflux transporters were strongly enriched (12-fold enrichment, hypergeometric p 0.002). Interestingly, we additionally found several other maize genes predicted to be related to auxin within those differentially expressed in response to infection by the mutant or SG200.

Summary

In this study, the influence of different host genotypes on *U. maydis* virulence was investigated, which revealed that activity and function of effector genes are specifically dependent on the host line. A maize line-specific virulence function was identified for the effector gene UMAG_02297, and transcriptome data suggested auxin-related processes as a possible target of this effector. Since targets of pathogen effectors that quantitatively contribute to virulence are potential candidates involved in QDR, further functional characterisation of the identified maize line-specific effector will provide more insights into the molecular mechanisms underlying QDR in the maize-*U. maydis* interaction and how *U. maydis* interferes with them.

Acknowledgements

Selma Schurack received support by the International Max Planck Research School of the MPIPZ, Cologne, Germany. This work was funded by the European Research Council under the European Union's Horizon 2020 research and innovation programme (consolidator grant conVIRgens, ID771035), as well as funding by the Deutsche Forschungsgemeinschaft (German Research Foundation [DFG]) under Germany's Excellence Strategy (EXC-2048/1–Project ID: 390686111). We are grateful to Benjamin Stich for generously supplying Ky21and Tx303 seeds, to Elaine Jaeger for helping with the initial acquirement of NAM founder lines and to Mariana Schuster for providing *U.maydis* strains. We thank Henriette Läßle for excellent help with the project. We acknowledge the Cologne Center for Genomics (Cologne, Germany) for sequencing support. This work is published in Schurack et al. (2021).

Literature

Basse, C. W., & Steinberg, G. (2004). Ustilago maydis, model system for analysis of the molecular basis of fungal pathogenicity. *Molecular Plant Pathology*, *5*(2), 83–92. https://doi.org/10.1111/j.1364-3703.2004.00210.x

Dutheil, J. Y., Mannhaupt, G., Schweizer, G., Sieber, C. M. K., Münsterkötter, M., Güldener, U., … Kahmann, R. (2016). A tale of genome compartmentalization: The evolution of virulence clusters in smut fungi. *Genome Biology and Evolution*, *8*(3), 681–704. https://doi.org/10.1093/gbe/evw026

Hoover, M. M. (1932). Inheritance Studies of the Reaction to Selfed Lines of Maize to Smut (Ustilago Zeae). *West Virginia Agricultural and Forestry Experiment Station Bulletins*, *253*.

Immer, F. (1927). The Inheritance of Reaction to Ustilago Zeae in Maize. *University of Minnesota Agricultural Experiment Station Technical Bulletin*, *51*(October).

Kämper, J., Kahmann, R., Bölker, M., Ma, L.-J., Brefort, T., Saville, B. J., … Birren, B. W. (2006). Insights from the genome of the biotrophic fungal plant pathogen Ustilago maydis. *Nature*, *444*(7115), 97–101. https://doi.org/10.1038/nature05248

Redkar, A., & Doehlemann, G. (2016). Ustilago maydis Virulence Assays in Maize. *Bio-Protocol*, *6*(6), e1760. https://doi.org/10.21769/BioProtoc.1760

Schurack, S., Depotter, J. R. L., Gupta, D., Thines, M., & Doehlemann, G. (2021). Comparative transcriptome profiling identifies maize line specificity of fungal effectors in the maize–Ustilago maydis interaction. *Plant Journal*, *106*(3), 733–752. https://doi.org/10.1111/tpj.15195

Schuster, M., Schweizer, G., Reissmann, S., & Kahmann, R. (2016). Genome editing in Ustilago maydis using the CRISPR-Cas system. *Fungal Genetics and Biology*, *89*, 3–9. https://doi.org/10.1016/j.fgb.2015.09.001

Stirnberg, A., & Djamei, A. (2016). Characterization of ApB73, a virulence factor important for colonization of Zea mays by the smut Ustilago maydis. *Molecular Plant Pathology*, *17*(9), 1467–1479. https://doi.org/10.1111/mpp.12442